9) Kondo T, Asai M, Tsukita K, Kutoku Y, Ohsawa Y, Sunada Y, et al.: Modeling Alzheimer's disease with iPSCs reveals stress phenotypes associated with intracellular Aβ and differential drug responsiveness. Cell Stem Cell 2013; 12: 487–496.
10) Israel MA, Yuan SH, Bardy C, Reyna SM, Mu Y, Herrera C, et al.: Probing sporadic and familial Alzheimer's disease using induced pluripotent stem cells. Nature 2012; 482: 216–220.
11) Yahata N, Asai M, Kitaoka S, Takahashi K, Asaka I, Hioki H, et al.: Anti-Aβ drug screening platform using human iPS cell-derived neurons for the treatment of Alzheimer's disease. PLoS One 2011; 6: e25788.
12) Mertens J, Stüber K, Wunderlich P, Ladewig J, Kesavan JC, Vandenberghe R, et al.: APP Processing in Human Pluripotent Stem Cell-Derived Neurons Is Resistant to NSAID-Based γ-Secretase Modulation. Stem Cell Reports 2013; 1: 491–498.
13) Ling SC, Polymenidou M, Cleveland DW: Converging mechanisms in ALS and FTD: disrupted RNA and protein homeostasis. Neuron 2013; 79: 416–438.
14) Fong H, Wang C, Knoferle J, Walker D, Balestra ME, Tong LM, et al.: Genetic correction of tauopathy phenotypes in neurons derived from human induced pluripotent stem cells. Stem Cell Reports 2013; 1: 226–334.
15) Egawa N, Kitaoka S, Tsukita K, Naitoh M, Takahashi K, Yamamoto T, et al.: Drug screening for ALS using patient-specific induced pluripotent stem cells. Sci Transl Med 2012; 4: 145ra104.
16) Alami NH, Smith RB, Carrasco MA, Williams LA, Winborn CS, Han SS, et al.: Axonal transport of TDP-43 mRNA granules is impaired by ALS-causing mutations. Neuron 2014; 81: 536–543.
17) Almeida S, Gascon E, Tran H, Chou HJ, Gendron TF, Degroot S, et al.: Modeling key pathological features of frontotemporal dementia with C9ORF72 repeat expansion in iPSC-derived human neurons. Acta Neuropathol 2013; 126: 385–399.
18) Donnelly CJ, Zhang PW, Pham JT, Heusler AR, Mistry NA, Vidensky S, et al.: RNA toxicity from the ALS/FTD C9ORF72 expansion is mitigated by antisense intervention. Neuron 2013; 80: 415–428.
19) Sareen D, O'Rourke JG, Meera P, Muhammad AK, Grant S, Simpkinson M, et al.: Targeting RNA foci in iPSC-derived motor neurons from ALS patients with a C9ORF72 repeat expansion. Sci Transl Med 2013; 5: 208 ra149.
20) Wainger BJ, Kiskinis E, Mellin C, Wiskow O, Han SS, Sandoe J, et al.: Intrinsic membrane hyperexcitability of amyotrophic lateral sclerosis patient-derived motor neurons. Cell Rep 2014; 7: 1–11.
21) Kiskinis E, Sandoe J, Williams LA, Boulting GL, Moccia R, Wainger BJ, et al.: Pathways Disrupted in Human ALS Motor Neurons Identified through Genetic Correction of Mutant SOD1. Cell Stem Cell 2014; 14: 1–15.
22) Vekrellis K, Xilouri M, Emmanouilidou E, Rideout HJ, Stefanis L: Pathological roles of α-synuclein in neurological disorders. Lancet Neurol 2011; 10: 1015–1025.
23) Meeus B, Theuns J, Van Broeckhoven C: The genetics of dementia with Lewy bodies: what are we missing? Arch Neurol 2012; 69: 1113–1118.
24) Chung CY, Khurana V, Auluck PK, Tardiff DF, Mazzulli JR, Soldner F, et al.: Identification and rescue of α-synuclein toxicity in Parkinson patient-derived neurons. Science 2013; 342: 983–987.
25) Mazzulli JR, Xu YH, Sun Y, Knight AL, McLean PJ, Caldwell GA, et al.: Gaucher disease glucocerebrosidase and α-synuclein form a bidirectional pathogenic loop in synucleinopathies. Cell 2011; 146: 37–52.
26) Sánchez-Danés A, Richaud-Patin Y, Carballo-Carbajal I, Jiménez-Delgado S, Caig C, Mora S, et al.: Disease-specific phenotypes in dopamine neurons from human iPS-based models of genetic and sporadic Parkinson's disease. EMBO Mol Med 2012; 4: 380–395.
27) Chang T, Zheng W, Tsark W, Bates S, Huang H, Lin RJ, et al.: Brief report: phenotypic rescue of induced pluripotent stem cell-derived motoneurons of a spinal muscular atrophy patient. Stem Cells 2011; 29: 2090–2093.
28) Byers B, Cord B, Nguyen HN, Schüle B, Fenno L, Lee PC, et al.: SNCA triplication Parkinson's patient's iPSC-derived DA neurons accumulate α-synuclein and are susceptible to oxidative stress. PLoS One 2011; 6: e26159.
29) Nguyen HN, Byers B, Cord B, Shcheglovitov A, Byrne J, Gujar P, et al.: LRRK2 mutant iPSC-derived DA neurons demonstrate increased susceptibility to oxidative stress. Cell Stem Cell 2011; 8: 267–280.
30) Seibler P, Graziotto J, Jeong H, Simunovic F, Klein C, Krainc D: Mitochondrial Parkin recruitment is impaired in neurons derived from mutant PINK1 induced pluripotent stem cells. J Neurosci 2011; 31: 5970–5976.
31) Soldner F, Laganiére J, Cheng AW, Hockemeyer D, Gao Q, Alagappan R, et al.: Generation of isogenic pluripotent stem cells differing exclusively at two early onset Parkinson point mutations. Cell 2011; 146: 318–331.
32) Cooper O, Seo H, Andrabi S, Guardia-Laguarta C, Graziotto J, Sundberg M, et al.: Pharmacological rescue of mitochondrial deficits in iPSC-derived neural cells from patients with familial Parkinson's disease. Sci Transl Med 2012; 4: 141ra90.
33) Imaizumi Y, Okada Y, Akamatsu W, Koike M, Kuzumaki N, Hayakawa H, et al.: Mitochondrial dysfunction associated with increased oxidative stress and α-synuclein accumulation in PARK2 iPSC-derived neurons and postmortem brain tissue. Mol Brain 2012; 5: 35.
34) Orenstein SJ, Kuo SH, Tasset I, Arias E, Koga H, Fernandez-Carasa I, et al.: Interplay of LRRK2 with chaperone-mediated autophagy. Nat Neurosci 2013; 16: 394–406.
35) Reinhardt P, Schmid B, Burbulla LF, Schöndorf DC, Wagner L, Glatza M, et al.: Genetic correction of a LRRK2 mutation in human iPSCs links parkinsonian neurodegeneration to ERK-dependent changes in gene expression. Cell Stem Cell 2013; 12: 354–367.
36) Sanders LH, Laganière J, Cooper O, Mak SK, Vu BJ, Huang YA, et al.: LRRK2 mutations cause mitochondrial DNA damage in iPSC-derived neural cells from Parkin-

son's disease patients: reversal by gene correction. Neurobiol Dis 2014; 62: 381–386.
37) Panicker LM, Miller D, Park TS, Patel B, Azevedo JL, Awad O, et al.: Induced pluripotent stem cell model recapitulates pathologic hallmarks of Gaucher disease. Proc Natl Acad Sci U S A 2012; 109: 18054–18059.
38) Denton KR, Lei L, Grenier J, Rodionov V, Blackstone C, Li XJ: Loss of spastin function results in disease-specific axonal defects in human pluripotent stem cell-based models of hereditary spastic paraplegia. Stem Cells 2014; 32: 414–423.
39) Havlicek S, Kohl Z, Mishra HK, Prots I, Eberhardt E, Denguir N, et al.: Gene dosage-dependent rescue of HSP neurite defects in SPG4 patients' neurons. Hum Mol Genet 2014; 23: 2527–2541.
40) Lee G, Papapetrou EP, Kim H, Chambers SM, Tomishima MJ, Fasano CA, et al.: Modelling pathogenesis and treatment of familial dysautonomia using patient-specific iPSCs. Nature 2009; 461: 402–406.
41) Lee G, Ramirez CN, Kim H, Zeltner N, Liu B, Radu C, et al.: Large-scale screening using familial dysautonomia induced pluripotent stem cells identifies compounds that rescue IKBKAP expression. Nat Biotechnol 2012; 30: 1244–1248.
42) Nihei Y, Ito D, Okada Y, Akamatsu W, Yagi T, Yoshizaki T, et al.: Enhanced aggregation of androgen receptor in induced pluripotent stem cell-derived neurons from spinal and bulbar muscular atrophy. J Biol Chem 2013; 288: 8043–8052.
43) Sheridan SD, Theriault KM, Reis SA, Zhou F, Madison JM, Daheron L, et al.: Epigenetic characterization of the FMR1 gene and aberrant neurodevelopment in human induced pluripotent stem cell models of fragile X syndrome. PLoS One 2011; 6: e26203.
44) Liu J, Koscielska KA, Cao Z, Hulsizer S, Grace N, Mitchell G, et al.: Signaling defects in iPSC-derived fragile X premutation neurons. Hum Mol Genet 2012; 21: 3795–3805.
45) Xia G, Santostefano K, Hamazaki T, Liu J, Subramony SH, Terada N, et al.: Generation of human-induced pluripotent stem cells to model spinocerebellar ataxia type 2 in vitro. J Mol Neurosci 2013; 51: 237–248.
46) Koch P, Breuer P, Peitz M, Jungverdorben J, Kesavan J, Poppe D, et al.: Excitation-induced ataxin-3 aggregation in neurons from patients with Machado-Joseph disease. Nature 2011; 480: 543–546.
47) Shi Y, Kirwan P, Smith J, MacLean G, Orkin SH, Livesey FJ: A human stem cell model of early Alzheimer's disease pathology in Down syndrome. Sci Transl Med 2012; 4: 124ra29.
48) Weick JP, Held DL, Bonadurer GF 3rd, Doers ME, Liu Y, Maguire C, et al.: Deficits in human trisomy 21 iPSCs and neurons. Proc Natl Acad Sci U S A 2013; 110: 9962–9967.
49) Paşca SP, Portmann T, Voineagu I, Yazawa M, Shcheglovitov A, Paşca AM, et al.: Using iPSC-derived neurons to uncover cellular phenotypes associated with Timothy syndrome. Nat Med 2011; 17: 1657–1662.
50) Krey JF, Paşca SP, Shcheglovitov A, Yazawa M, Schwemberger R, Rasmusson R, et al.: Timothy syndrome is associated with activity-dependent dendritic retraction in rodent and human neurons. Nat Neurosci 2013; 16: 201–209.
51) Higurashi N, Uchida T, Lossin C, Misumi Y, Okada Y, Akamatsu W, et al.: A human Dravet syndrome model from patient induced pluripotent stem cells. Mol Brain 2013; 6: 19.
52) Liu Y, Lopez-Santiago LF, Yuan Y, Jones JM, Zhang H, O'Malley HA, et al.: Dravet syndrome patient-derived neurons suggest a novel epilepsy mechanism. Ann Neurol 2013; 74: 128–139.
53) Trilck M, Hübner R, Seibler P, Klein C, Rolfs A, Frech MJ: Niemann-Pick type C1 patient-specific induced pluripotent stem cells display disease specific hallmarks. Orphanet J Rare Dis 2013; 8: 144.
54) Zhang N, An MC, Montoro D, Ellerby LM: Characterization of Human Huntington's Disease Cell Model from Induced Pluripotent Stem Cells. PLoS Curr 2010; 2: RRN 1193.
55) Camnasio S, Delli Carri A, Lombardo A, Grad I, Mariotti C, et al.: The first reported generation of several induced pluripotent stem cell lines from homozygous and heterozygous Huntington's disease patients demonstrates mutation related enhanced lysosomal activity. Neurobiol Dis 2012; 46: 41–51.
56) Jeon I, Lee N, Li JY, Park IH, Park KS, Moon J, et al.: Neuronal properties, in vivo effects, and pathology of a Huntington's disease patient-derived induced pluripotent stem cells. Stem Cells 2012; 30 (9): 2054–2062.
57) Chae JI, Kim DW, Lee N, Jeon YJ, Jeon I, Kwon J, et al.: Quantitative proteomic analysis of induced pluripotent stem cells derived from a human Huntington's disease patient. Biochem J 2012; 446: 359–371.
58) An MC, Zhang N, Scott G, Montoro D, Wittkop T, Mooney S, et al.: Genetic correction of Huntington's disease phenotypes in induced pluripotent stem cells. Cell Stem Cell 2012; 11: 253–263.
59) HD iPSC Consortium: Induced pluripotent stem cells from patients with Huntington's disease show CAG-repeat-expansion-associated phenotypes. Cell Stem Cell 2012; 11: 264–278.
60) Jang J, Kang HC, Kim HS, Kim JY, Huh YJ, Kim DS, et al.: Induced pluripotent stem cell models from X-linked adrenoleukodystrophy patients. Ann Neurol 2011; 70: 402–409.
61) Liu J, Verma PJ, Evans-Galea MV, Delatycki MB, Michalska A, Leung J, et al.: Generation of induced pluripotent stem cell lines from Friedreich ataxia patients. Stem Cell Rev 2011; 7: 703–713.
62) Du J, Campau E, Soragni E, Ku S, Puckett JW, Dervan PB, et al.: Role of mismatch repair enzymes in GAA・TTC triplet-repeat expansion in Friedreich ataxia induced pluripotent stem cells. J Biol Chem 2012; 287: 29861–29872.
63) Numasawa-Kuroiwa Y, Okada Y, Shibata S, Kishi N, Akamatsu W, Shoji M, et al.: Involvement of ER Stress in Dysmyelination of Pelizaeus-Merzbacher Disease with

PLP1 Missense Mutations Shown by iPSC-Derived Oligodendrocytes. Stem Cell Reports 2014; 2: 648–661.
64) Marchetto MC, Carromeu C, Acab A, Yu D, Yeo GW, Mu Y, et al.: A model for neural development and treatment of Rett syndrome using human induced pluripotent stem cells. Cell 2010; 143: 527–539.
65) Kim KY, Hysolli E, Park IH: Neuronal maturation defect in induced pluripotent stem cells from patients with Rett syndrome. Proc Natl Acad Sci U S A 2011; 108: 14169–14174.
66) Ananiev G, Williams EC, Li H, Chang Q: Isogenic pairs of wild type and mutant induced pluripotent stem cell (iPSC) lines from Rett syndrome patients as in vitro disease model. PLoS One 2011; 6: e25255.
67) Kuro-o M, Matsumura Y, Aizawa H, Kawaguchi H, Suga T, Utsugi T, et al.: Mutation of the mouse klotho gene leads to a syndrome resembling ageing. Nature 1997; 390: 45–51.
68) Takeda T: Senescence-accelerated mouse (SAM) with special references to neurodegeneration models, SAMP8 and SAMP10 mice. Neurochem Res 2009; 34: 639–659.
69) Prokocimer M, Barkan R, Gruenbaum Y: Hutchinson-Gilford progeria syndrome through the lens of transcription. Aging Cell 2013; 12: 533–543.
70) Miller JD, Ganat YM, Kishinevsky S, Bowman RL, Liu B, Tu EY, et al.: Human iPSC-based modeling of late-onset disease via progerin-induced aging. Cell Stem Cell 2013; 13: 691–705.
71) Bibikova M, Beumer K, Trautman JK, Carroll D: Enhancing gene targeting with designed zinc finger nucleases. Science 2003; 300: 764.
72) Mussolino C, Morbitzer R, Lütge F, Dannemann N, Lahaye T, Cathomen T: A novel TALE nuclease scaffold enables high genome editing activity in combination with low toxicity. Nucleic Acids Res 2011; 39: 9283–9293.
73) Hwang WY, Fu Y, Reyon D, Maeder ML, Tsai SQ, Sander JD, et al.: Efficient genome editing in zebrafish using a CRISPR-Cas system. Nat Biotechnol 2013; 31: 227–229.
74) Morris SA, Daley GQ: A blueprint for engineering cell fate: current technologies to reprogram cell identity. Cell Res 2013; 23: 33–48.
75) Sun CK, Zhou D, Zhang Z, He L, Zhang F, Wang X, et al.: Senescence impairs direct conversion of human somatic cells to neurons. Nat Commun 2014; 5: 4112.
76) Eiraku M, Watanabe K, Matsuo-Takasaki M, Kawada M, Yonemura S, Matsumura M, et al.: Self-organized formation of polarized cortical tissues from ESCs and its active manipulation by extrinsic signals. Cell Stem Cell 2008; 3: 519–532.
77) Kadoshima T, Sakaguchi H, Nakano T, Soen M, Ando S, Eiraku M, et al.: Self-organization of axial polarity, inside-out layer pattern, and species-specific progenitor dynamics in human ES cell-derived neocortex. Proc Natl Acad Sci U S A 2013; 110: 20284–20289.
78) Lancaster MA, Renner M, Martin CA, Wenzel D, Bicknell LS, Hurles ME, et al.: Cerebral organoids model human brain development and microcephaly. Nature 2013; 501: 373–379.

幹細胞を用いてシャーレの中で病気を再現できればほかの方法では手に入れるのが難しい，あるいはまったく入手不可能な細胞を実験に使う道が開ける

に30を超え，今も増え続けている。その多くは，極めて重篤なALS患者に見られる変異を持っている。

さらに重要なのは，シャーレ内で病気を再現するという手法の威力が発揮され始め，運動ニューロン病の本質についての手掛かりが得られつつあることだ。例えば，クロアチアの老姉妹の細胞を用いた研究から，運動ニューロンの死と関係があるとみられる分子経路が見つかった（論文では未発表。右ページの監修者ノート参照）。運動ニューロンは，ニューロンをサポートするアストロサイトと呼ばれるグリア細胞から放出される毒素にさらされると死滅する。現在，ニューロンとアストロサイトを同じシャーレで培養し，アストロサイトの毒性を阻害するか，あるいは運動ニューロンの生存を助ける物質の探索が進んでいる。

また2010年1月，プロジェクトALSは，ALS患者からiPS細胞技術で作り出した運動ニューロンを用いて，約2000の化合物の一次スクリーニングを始めた。ALS遺伝子が変異したニューロンの生存期間を延ばす分子がないかどうかを調べる。今回の予備的な計画は，薬剤スクリーニングにおける新しい考え方を取り入れている。ほかの病気の治療薬としてすでに米食品医薬品局（FDA）に認可されている薬剤から調べ始めたのだ。運が良ければ，すでにヒトでの安全性が試験され，確認されているものの中から目的の物質が見つかり，すぐさま運動ニューロン疾患に適用拡大できるだろう。

ルビンはハーバード大学で同様の研究を進め，プロジェクトALSが発見した分子経路の1つに作用して，運動ニューロンの生存期間を延長する低分子化合物を20種類以上見つけた。現在，脊髄性筋萎縮症財団が，この病気の動物モデルを用いてその1つを調べているところだ。

天からの蜘蛛の糸を生かすには

ベーブ・ルースと並んで，米メジャーリーグのニューヨーク・ヤンキースの顔だったルー・ゲーリックは，1938年に入り，プレーの精彩を極端に欠き始める。翌年，彼は，フランスの神経学者シャルコー（Jean-Martin Charcot）が1869年に記載した「脊髄が固くなる原因不明の麻痺」である筋萎縮性側索硬化症（amyotrophic lateral sclerosis：ALS）と診断されて引退を余儀なくされ，その2年後，37歳の若さで他界した。

それから70年たった現在，ALSは米国ではルー・ゲーリック病とも呼ばれているが，依然として有効な治療方法のない過酷な疾患であることに変わりはない。患者さんは症状の進行によって全身の運動機能を消失するが，進行後も，意識は清明で知的機能は保たれる。さらに，人工呼吸器を使用するか，そしてゴールのない介護を受けるかどうかという患者さんに突きつけられる選択は，ALSが最も容赦のない疾患の1つといわれる所以である。

1993年にALSの原因遺伝子の1つが同定され，さらにヒトと同様の症状を呈するモデルマウスが作出されたにもかかわらず，ALSの治療方法は確立していない。その解決のための重要なミッシングピースの1つがヒトの運動ニューロンであるという考えを，私たちのグループも有していた。そして米国のグループと同様，iPS細胞が発見される以前から，ALSの患者さんの皮膚にある幹細胞を収集し，運動ニューロンを作り出そうとしていた。米国のグループは核移植による方法を模索していたが，私たちは皮膚の幹細胞を運動ニューロンに分化させることに悪戦苦闘していた。

取り組んでいた方法は違えど，私たちにとっても，iPS細胞技術は天からの蜘蛛の糸であった。2008年夏，いよいよ患者さんの皮膚細胞から満を持してiPS細胞を作りはじめた1カ月後，私たちは，ALSの遺伝的特徴を持つ運動ニューロンを作り出したというエッガン博士らの論文に驚くことになる。

私たちを含め，この難問に取り組む世界中の研究者は，治療法の開発という最終ゴールのために，あらゆる可能性，考えうるすべての手法を導入しようとしている。さらに，分野を超えて協力しうるすべての研究者との共同研究によって，全速力で，疾患の制圧を目指している。

その中で，iPS細胞作成技術というこれまでの歴史上に存在しなかった革命的技術はどうしても必要であり，それを用いることによって，シャーレの中での難病の疾患モデリングが可能となるであろう。ALSだけではない。慢性乳児神経皮膚関節炎症候群，多発性嚢胞腎，ダウン症，脊髄性筋萎縮症，肺高血圧症をはじめ，ほかの多くの病気についても，シャーレ内で疾患モデルを作る研究が日本と世界で精力的に行われており，知見が蓄積されつつある。

iPS細胞を用いた研究は，既存のパラダイムとの融合によって，病態解明，創薬開発をさらに加速することになると思われる。与えられた蜘蛛の糸を最大限に生かし，いかに疾患の治療法につなげていくかが，今後の重要課題である。

（井上治久＝右ページの監修者紹介参照）

nature COMMUNICATIONS

ARTICLE

Received 27 Oct 2013 | Accepted 17 Mar 2014 | Published 24 Apr 2014

DOI: 10.1038/ncomms4678

Induction of pluripotency in human somatic cells via a transient state resembling primitive streak-like mesendoderm

Kazutoshi Takahashi[1,*], Koji Tanabe[1,*], Mari Ohnuki[1], Megumi Narita[1], Aki Sasaki[1], Masamichi Yamamoto[2], Michiko Nakamura[1], Kenta Sutou[1], Kenji Osafune[1] & Shinya Yamanaka[1,3]

During mammalian embryonic development, the primitive streak initiates the differentiation of pluripotent epiblast cells into germ layers. Pluripotency can be reacquired in committed somatic cells using a combination of a handful of transcription factors, such as OCT3/4, SOX2, KLF4 and c-MYC (hereafter referred to as OSKM), albeit with low efficiency. Here we show that during OSKM-induced reprogramming towards pluripotency in human cells, intermediate cells transiently show gene expression profiles resembling mesendoderm, which is a major component of the primitive streak. Based on these findings, we discover that forkhead box H1 (FOXH1), a transcription factor required for anterior primitive streak specification during early development, significantly enhances the reprogramming efficiency of human fibroblasts by promoting their maturation, including mesenchymal to epithelial transition and the activation of late pluripotency markers. These results demonstrate that during the reprogramming process, human somatic cells go through a transient state that resembles mesendoderm.

[1] Center for iPS cell Research and Application, Kyoto University, Kyoto 606-8507, Japan. [2] Development Unit, Gunma University Maebashi, Gunma 371-8511, Japan. [3] Gladstone Institute of Cardiovascular Disease, San Francisco, California 94158, USA. * These authors contributed equally to this work. Correspondence and requests for materials should be addressed to K.T. (email: takahash@cira.kyoto-u.ac.jp) or to S.Y. (email: yamanaka@cira.kyoto-u.ac.jp).

Ectopic expression of transcription factors including OCT3/4, SOX2, KLF4 and c-MYC (hereafter referred to as OSKM) can invoke latent pluripotency of differentiated somatic cells albeit at low efficiency[1,2]. The inefficiency of reprogramming has suggested that elimination of epigenetic barriers and/or undefined secondary events are required in addition to OSKM[3,4]. However, the contamination by non-reprogrammed cells, which is major component of reprogramming cultures, impedes the understanding of molecular mechanisms of reprogramming, since non-reprogrammed cells exhibit different characteristics including gene expression and epigenetic statuses from *bona fide* iPSCs. Therefore, it has been difficult to observe the truly significant events occurring only in the reprogrammed cells.

Recent works provided a concept of intermediate reprogrammed cell collection using specific cell surface antigens. Mouse intermediate reprogrammed cells can be labelled by stage-specific embryonic antigen (SSEA)-1 that is recognized as a specific marker of mouse embryonic stem cells (ESCs)/iPSCs[5–7]. We demonstrated that human cells positive (+) for tumor-related antigen (TRA)-1-60[8,9] induced by OSKM are intermediate reprogrammed cells to being iPSCs[10]. Behaviour of TRA-1-60 (+) intermediate reprogrammed cells suggested that maturation, but not the initiation step, is a bottleneck of cell fate conversion towards human iPSCs. However, little is known about the characteristics of intermediate reprogrammed cells.

In the current study, we purified TRA-1-60 (+) intermediate reprogrammed cells, which are candidates for *bona fide* iPSCs. Gene expression analyses revealed that mesendodermal genes are transiently activated during reprogramming, and re-suppressed in iPSCs. These findings led us discover that forkhead box H1 (FOXH1), a transcription factor that is essential for primitive streak specification, facilitates iPSC generation by promoting the maturation of intermediate reprogrammed cells including the mesenchymal to epithelial transition (MET) and the expression of marker genes for the late phase of reprogramming. These data demonstrate that the transient primitive streak-like mesendodermal (PSMN) state is crucial for the maturation of reprogrammed cells.

Results

The presence of large numbers of non-reprogrammed cells during the generation of iPSCs inhibits the accurate analysis of the reprogramming process. To overcome this issue, we used TRA-1-60 to capture cells being reprogrammed (Fig. 1a). Human dermal fibroblasts (HDFs) were transduced with OSKM retroviruses, transferred onto SNL feeder cells on day 7, and cultured under the conditions for ESCs thereafter. As part of our conventional protocol to generate iPSCs, we pick up colonies on around day 28 and continue cultivation for >20 passages to establish iPSC lines. In the current study, we analysed the proportion of TRA-1-60 (+) cells on various days by flow cytometry, and collected positive cells by using TRA-1-60 antibody-conjugated magnetic beads. A small population of TRA-1-60 (+) cells was detected on day 7, and then gradually increased in quantity and intensity (Fig. 1b, Supplementary Fig. 1). The ability of TRA-1-60 (+) cells to form iPSC colonies also gradually increased and reached an efficiency similar to that of ESCs/iPSCs on day 20 or 28 (Fig. 1c). These results demonstrated that TRA-1-60 (+) cells were being reprogrammed toward iPSCs.

In TRA-1-60 (+) cells, the expression of pluripotent stem cell markers, such as *NANOG* and endogenous *OCT3/4*, progressively increased (Fig. 1d and Supplementary Fig. 2). The transgene expression levels of the OSKM retroviruses peaked during day 7 and 15, and then became silenced by day 28 (Supplementary Fig. 3). These data confirmed the gradual progression of reprogramming in TRA-1-60 (+) cells. Unexpectedly, however, we found that several pluripotent stem cell marker genes, such as *GDF3*, *LEFTY2* and *NODAL*, showed much higher expression levels in TRA-1-60 (+) cells than in iPSCs or ESCs (Fig. 1d and Supplementary Fig. 2). This may suggest that TRA-1-60 (+) cells enter a transient state during reprogramming.

To further explore this possibility, we compared the global gene expression profiles of TRA-1-60 (+) cells purified on various days, original HDFs, established iPSCs and differentiated progenies (endoderm, EN; mesoderm, ME; neuroectoderm, NE; and primitive streak-like mesendoderm[11–14], PSMN from ESCs/iPSCs using DNA microarrays (Supplementary Fig. 4). The principle component analysis (PCA) revealed that the expression levels of significant number of genes in TRA-1-60 (+) cells were not intermediate between HDFs and iPSCs, but were transiently activated or suppressed during iPSC generation (Component 1 in Fig. 2a). The gene ontology analyses demonstrated that many of the transiently downregulated genes were related to metabolic processes (Supplementary Fig. 5)[15]. On the other hand, many of the transiently activated genes were related to developmental processes (Supplementary Fig. 5).

The PCA and the hierarchical clustering demonstrated that that TRA-1-60 (+) cells on days 20–49 were most similar to mesendodermal cells derived from iPSCs, rather than undifferentiated iPSCs (Fig. 2a,b). The correlation coefficient of the global gene expression between TRA-1-60 (+) cells on day 20 and PSMN was 0.9718, which was comparable with clonal variations among ESC/iPSC lines (0.9634–0.9862) (Supplementary Tables 1 and 2). In addition, we extended our comparison to 24 human fetal or adult tissues, and eight tissue-derived cells, in addition to the four ESC/iPSC-derived differentiated cells (Supplementary Fig. 6). The highest similarity was observed between TRA-1-60 (+) cells (days 20–49) and PSMN.

Approximately 40% of the PSMN-enriched genes were included in the transiently upregulated genes in TRA-1-60 (+) cells (Fig. 2c). We then checked the expression levels of marker genes for various developmental lineages. Marker genes for primitive streak, such as *BRACHYURY* (*T*), *MIXL1*, *CER1*, *LHX1* and *EOMES* showed a transient activation during iPSC generation in TRA-1-60 (+) cells (Fig. 2d). In contrast, marker genes for other lineages, including pluripotent stem cells, ME, EN and neuroectoderm, did not show such transient changes (Supplementary Fig. 7). Quantitative reverse transcription polymerase chain reaction confirmed the transient activation of primitive streak-related genes in TRA-1-60 (+) cells (Fig. 2e, Supplementary Fig. 8). The occupancy of trimethylated lysine 4 of histone H3 (H3K4me3), which is a mark of an activated promoter, transiently increased in primitive streak-related gene loci during reprogramming (Fig. 2e, Supplementary Fig. 8). Single-cell quantitative reverse transcription polymerase chain reaction and immunocytochemistry revealed that virtually all of TRA-1-60 (+) cells on day 20, but not HDFs or ESCs, expressed T (Fig. 2f,g). These data suggest that TRA-1-60 (+) cells possess gene expression profiles resembling PSMN during the late stage of reprogramming.

TRA-1-60 (+) cells induced by OSKM, along with GLIS1 or short hairpin RNA (shRNA)-mediated depletion of *p53* (p53 shRNA), two of the strongest enhancers of reprogramming, were also clustered with PSMN (Fig. 2h)[16–21]. In addition, TRA-1-60 (+) cells derived from adipose-derived stem cells (ASC), as well as non-mesodermal lineages, such as astrocytes (HA, ectoderm), bronchial epithelium (NHBE, EN) and prostate epithelial cells (PrEC, EN), showed similarities to the PSMN in terms of the global gene expression (Fig. 2i and Supplementary Fig. 9). Therefore, nascent human reprogrammed cells exhibit PSMN features, regardless of the reprogramming factors used or germ layer of original human somatic cells.

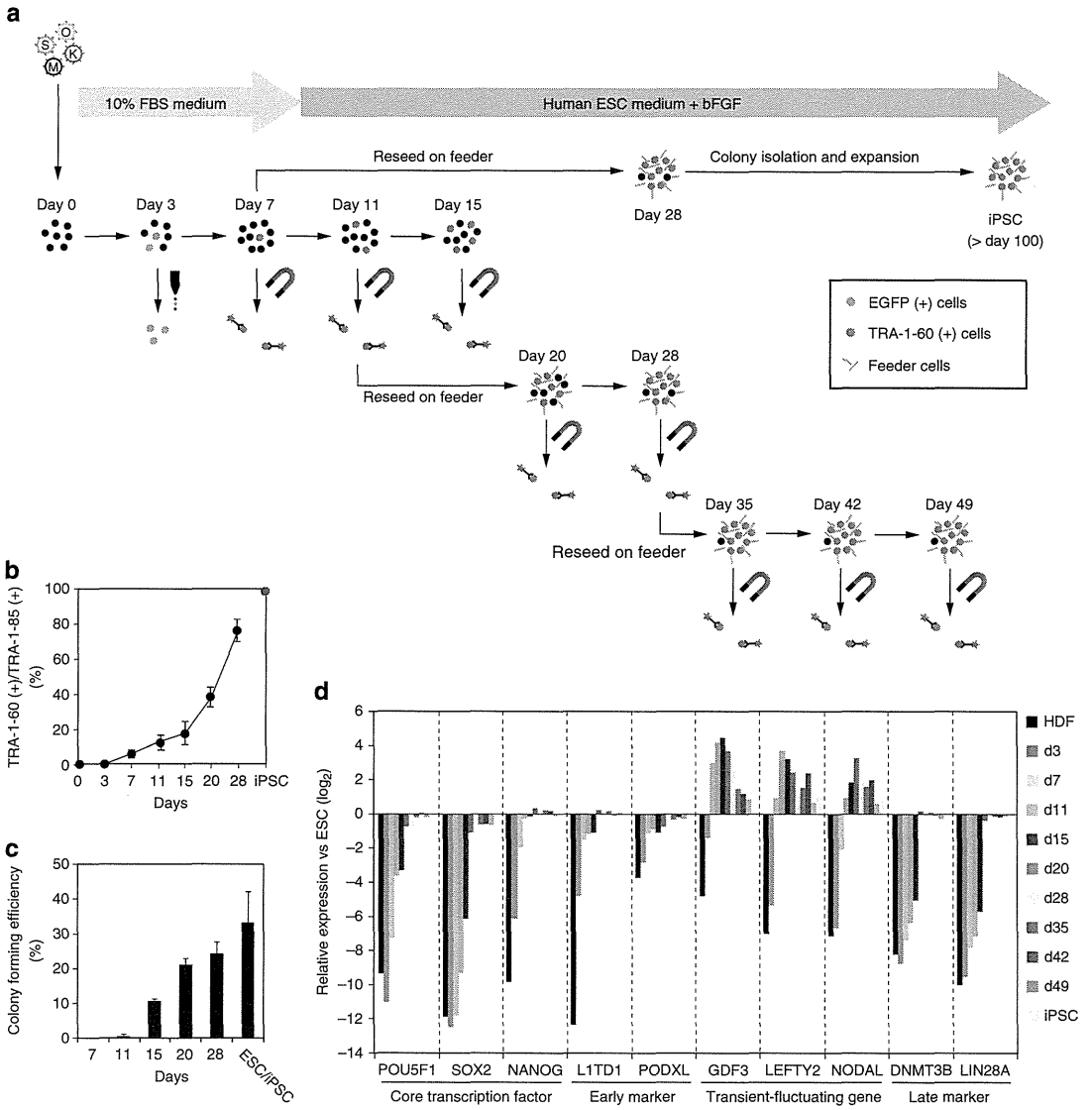

Figure 1 | TRA-1-60 (+) cells as an origin of human iPSCs. (**a**) A schematic drawing of TRA-1-60 (+) intermediate cells throughout human cellular reprogramming. (**b**) The proportion of TRA-1-60 (+) cells in human reprogramming cultures. Shown are the average proportions of TRA-1-60 (+) cells expressing TRA-1-85, which is a pan-human cell marker. $N=3$. (**c**) The efficiencies of iPSC generation from single TRA-1-60 (+) cells at each time point. The colony forming efficiencies were estimated by the number of iPSC colony-formed wells in single TRA-1-60 (+) cell sorted 96-well plates. $N=3$. (**d**) The expression of pluripotency-associated genes in TRA-1-60 (+) cells. The mean expressions from three microarray data sets for each time point, normalized to the levels of ESCs are shown.

The hierarchical clustering demonstrated that the TRA-1-60 (+) cells in early phases of reprogramming (days 3–15) resembled epithelial cells, including epidermis (EDM), PrEC and NHBE (green box in Supplementary Fig. 6). The correlation coefficient between TRA-1-60 (+) cells on days 3–15 and EDM, PrEC and NHBE were 0.9082–0.9105, 0.8989–0.9052 and 0.9033–0.9106, respectively (Supplementary Table 3). We also observed suppression of mesenchymal genes and activation of epithelial genes during this period[22,23] (Supplementary Fig. 10). Taken together, these data suggest that epithelialization is one of the dominant events that occur in TRA-1-60 (+) intermediate cells during the early phases of reprogramming. This result may explain a recent report arguing that there was a transient EDM-like status during mouse cell reprogramming[6].

Our findings led us to hypothesize that transcription factors that play important roles in mesendoderm and primitive streak may facilitate iPSC generation. We selected 23 transcription factors that were highly expressed in mesendoderm and transduced each one of them, together with OSKM, into HDFs (Fig. 3a). We found that five factors, including FOXA2, FOXF1, FOXH1, LHX1 and T, significantly increased the numbers of iPSC colonies. Among them, FOXH1 showed the strongest effect. FOXH1 functions as a downstream target of the Nodal signal and is required for the specification of anterior primitive streak[24,25]. The effect of FOXH1 in increasing iPSC colonies was comparable with those of p53 shRNA and GLIS1 (Fig. 3b and Supplementary Fig. 11)[16–21].

We previously reported that mouse *Glis1* was specifically expressed in unfertilized oocytes in mice, and that it facilitated iPSC generation through promoting the expression of pluripotency-associated genes[26]. In this study, we found that *GLIS1* was highly expressed in PSMN derived from human ESCs/iPSCs

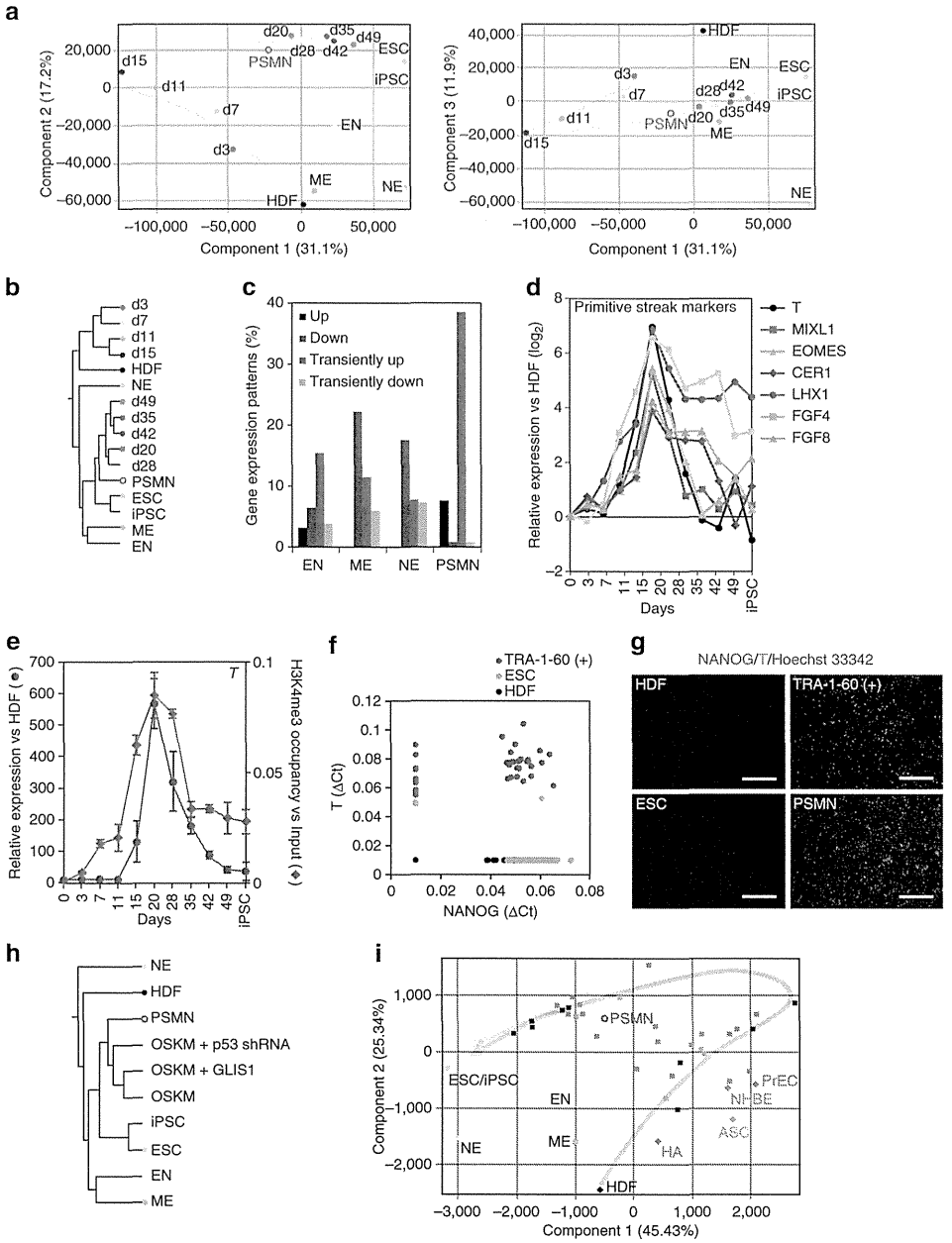

Figure 2 | The transient mesendodermal status of intermediate reprogrammed cells. (**a**) Comparison of the global gene expression between TRA-1-60 (+) cells and germ layers. Shown are PCA of the global gene expression in parental HDFs, TRA-1-60 (+) cells at the indicated time points, ESCs/iPSCs and differentiated cells, such as PSMN, EN, ME and NE. (**b**) Shown are the hierarchical clustering results of the global gene expression in parental HDFs, TRA-1-60 (+) cells at the indicated time points, ESCs/iPSCs and differentiated cells, such as PSMN, EN, ME and NE. (**c**) PSMN-enriched genes transiently upregulated in TRA-1-60 (+) cells. Shown are the percentages of ever-upregulated (black), ever-downregulated (blue), transiently upregulated (red) and transiently downregulated (green) genes in the enriched genes of PSMN, EN, ME or NE. (**d**) The expression of representative primitive streak marker genes during reprogramming. Shown are the relative expression levels of selected marker genes in TRA-1-60 (+) cells compared with parental HDFs. In these analyses, the averages of three microarray data set for each sample were used. (**e**) The expression and active histone marks of *T* gene during reprogramming. Blue circles indicate the relative expression of *T* compared with that in HDFs. Red diamonds indicate the occupancy of H3K4me3 at the promoter region of *T* gene. $N=3$. (**f**) The single-cell expression of *T*. The expression of *NANOG* and *T* in single HDFs and TRA-1-60 (+) cells on day 20 and ESCs. Each dot indicates one cell sample. The relative expression levels are shown as the ΔCt from qPCR. (**g**) Immunocytochemistry of T protein. The expression of NANOG (red) and T (green) in HDFs, TRA-1-60 (+) cells on day 20, ESCs and ESC-derived PSMN were analysed by immunocytochemistry. Nuclei were visualized by staining with Hoechst 33,342 (blue). Scale bars indicate 100 μm. (**h**) Booster-supported reprogramming via primitive streak-like state. The results of the hierarchical clustering analysis of the global gene expression in parental HDFs are shown, TRA-1-60 (+) cells on day 20 following transduction with OSKM, OSKM + GLIS1 and OSKM + p53 shRNA, ESCs/iPSCs and differentiated cells such as PSMN, EN, ME and NE. (**i**) The PCA of the microarray expression data from TRA-1-60 (+) cells at each time point, parental cell lines (HDF, HA, ASC, NHBE and PrEC), ESCs/iPSCs and differentiated cells such as PSMN, EN, ME and NE. Each arrow indicates the putative direction of the reprogramming progression.

(Supplementary Fig. 12a). We also found that mouse *Glis1* is expressed in embryonic regions, including primitive streak (Supplementary Fig. 12b). Forced expression of GLIS1 in human ESCs gave rise to PSMN features (Supplementary Fig. 12c,d,e). These data demonstrated that GLIS1 has important roles in the PSMN lineage, which may contribute to its pro-reprogramming activity.

In addition, the stage-specific activation of FOXH1 demonstrated that FOXH1 clearly facilitated the reprogramming efficiency in late stages (Fig. 3c). These results are in contrast to those using GLIS1, which facilitated reprogramming in the earlier stages and increased the proportion of TRA-1-60 (+) cells (Fig. 3d,e). This may suggest that GLIS1 promotes the induction of a primitive streak-like state, whereas FOXH1 promotes the maturation of cells in this state. In fact, the proportion of TRA-1-60 (+) cells was reproducibly reduced by FOXH1 on day 7, but the proportion was increased again on days 11 and 15 compared with cells transduced with OSKM alone (Fig. 3e). We found that FOXH1 promoted the downregulation of a fibroblast marker, CD13, and the upregulation of an epithelial marker, EpCAM, in TRA-1-60 (+) cells on days 11 and 15 (Fig. 3f). In addition, the expression of late reprogramming markers, such as *DPPA4*, *DNMT3B*, *LIN28A*, *ZFP42* and endogenous *SOX2* (ref. 7), were significantly enhanced by FOXH1 (Fig. 3g). These data further suggest that FOXH1 may enhance the reprogramming efficiency by facilitating the maturation of TRA-1-60 (+) cells.

Next, we examined whether endogenous FOXH1 is required for human iPSC generation and PSMN differentiation. Knockdown of *FOXH1* in ESCs significantly interfered with their differentiation into PSMN (Fig. 3h). The expression of endogenous *FOXH1* was continuously increased in TRA-1-60 (+) cells during their reprogramming towards iPSCs (Fig. 3i). Three out of six shRNAs (1, 3 and 6) suppressed the expression of endogenous *FOXH1* in ESCs or OSKM-transduced HDFs with ~90%, 70% and 50% efficiencies, respectively (Fig. 3i and Supplementary Fig. 13). When co-introduced with OSKM, shRNA1 nearly abolished the generation of iPSC colonies (Fig. 3j). In addition, shRNA 3 decreased iPSC colony formation by 50%. In contrast, the suppression of *FOXH1* did not ameliorate the proliferation of transduced HDFs (Fig. 3k). These data suggest that FOXH1 plays an important role in the reprogramming process towards iPSCs.

We then examined the effects of other FOX family transcription factors on human iPSC generation. We found that five factors, including FOXA2, FOXB1, FOXF1, FOXG1 and FOXH1, out of 36 selected FOX genes significantly increased the numbers of iPSC colonies (Supplementary Fig. 14). Similar to SOX, KLF and MYC families[27], some of FOX family transcription factors have overlapping effects on human iPSC generation (Supplementary Fig. 15). The use of FOXH1 along with OSKM for reprogramming did not alter the characteristics of the resulting iPSCs (Supplementary Fig. 16).

We examined whether mouse reprogramming also goes through a transient state. We reprogrammed mouse embryonic fibroblasts (MEFs) derived from Nanog-GFP transgenic mice[28], and isolated nascent reprogrammed cells as SSEA-1 (+) and/or Nanog-GFP (+). The PCA and hierarchical clustering of the microarray data identified a component that indicates a transient change resembling PSMN during mouse iPSC generation (Supplementary Fig. 17). In addition, by using a secondary iPSC induction system in mice, Polo *et al.*[5] reported that there was a transient activation of several genes, including *T*, *Eomes* and *Mixl1*.

Discussion

In summary, our cell capture strategy for human intermediate reprogrammed cells revealed that they go through a transient state that resembles PSMN. During the maturation step, virtually all TRA-1-60 (+) cells expressed early mesendodermal genes. Such PSMN features gradually drained in further progression of reprogramming towards iPSC. Previous and our current study clearly show that the human reprogramming process takes more time than we thought it would and the maturation step is important[29]. Although we have little evidence for the inevitability of the transition, this observation led us to find FOXH1 as an enhancer of reprogramming.

FOXH1 promoted the MET of TRA-1-60 (+) cells and the activation of late pluripotent markers. The epithelial to mesenchymal transition, which is an opposite phenomenon of MET, is a key event for differentiation of epiblasts into mesendoderm at primitive streak in embryonic development. FOXH1 may facilitate the reprogramming by promoting the reversion of somatic cell fate to PSMN state. Further understanding of the reprogramming process will enable more robust generation of human iPSCs.

Methods

Statistical analyses. We evaluated the data by paired *t*-tests using the Kaleidagraph software programme (HULINKS), and values of $P<0.05$ were considered to be significant (indicated by asterisks in figures). The error bars represent the standard deviation (s.d.).

Cell culture. We obtained HDFs from the Japanese Collection of Research Bioresources. HDFs, PLAT-E[30], PLAT-GP and MEFs were maintained in Dulbecco's modified Eagle medium (DMEM, Nacalai Tesque) containing 10% fetal bovine serum (FBS, Japan Bio Serum) and 0.5% penicillin and streptomycin (Pen/Strep, Life Technologies). ESC clones obtained from WiCELL[31] and Kyoto University[32] were maintained in Primate ESC medium (ReproCELL) supplemented with 4 ng ml^{-1} recombinant human basic fibroblast growth factor (bFGF, Wako) on mitomycin C (MMC)-inactivated SNL feeders[33], or in mTeSR1 (Veritas) on Matrigel-coated plates (growth factor reduced, BD biosciences) as described previously[2]. Human epidermal keratinocytes (EDM, Lonza), astrocytes (HA, Cell applications), normal human bronchial epithelial cells (NHBE, Lonza), adipose tissue-derived stem cells (ASC, Life Technologies) and prostate epithelial cells (PrEC, Lonza) were maintained under the manufacturer's recommended conditions.

Mouse ESCs (1B4) and iPSCs (20D17)[28] were maintained in mESC medium consisting of 80% knockout DMEM (Life Technologies), 15% knockout serum replacement (KSR, Life Technologies), 1% Glutamax, 1% NEAA, 100 nM 2-ME, 0.5% Pen/Strep and 1,000 units ml^{-1} recombinant mouse leukaemia inhibitory factor (Millipore) on gelatinized plates.

Reprogramming. To generate retroviral particles, we introduced retroviral vectors into PLAT-E or PLAT-GP cells by using the FuGENE 6 transfection reagent (Roche) as per the manufacturer's protocol. On the following day, the medium was replaced with fresh one and cells were incubated for another 24 h. The virus-containing supernatant was collected, filtered through a 0.45 μm pore size cellulose acetate filter (Whatman) and was supplemented with 4 μg ml^{-1} Polybrene (Nacalai Tesque). Then, we mixed appropriate combinations of viruses and used them to expose HDFs carrying the mouse Solute carrier family 7 (cationic amino-acid transporter, y+ system) member 1 (*Slc7a1*) gene overnight. This point was designated as day 0.

For the transduction of retroviruses into cell lines other than HDFs, we performed spinfection at 700*g* for 1 h with the fusiogenic envelope G glycoprotein of the vesicular stomatitis virus (VSV-G)-pseudotyped pantropic viruses produced by PLAT-GP cells. To collect the samples on day 3 post transduction, we introduced pMXs-IRES-EGFP (IG) encoding SOX2 instead of pMXs-SOX2, along with OKM, and sorted EGFP (+) cells by flow cytometry. We harvested the cells on day 7 post transduction, and re-plated them onto MMC-inactivated SNL feeders to generate iPSCs. The following day, the medium was replaced with Primate ESC medium supplemented with 4 ng ml^{-1} bFGF, and the medium was changed every other day. To collect TRA-1-60 (+) cells, we performed magnetic-activated cell sorting with a TRA-1-60 antibody at each indicated time point. The number of iPSC colonies was counted on day 24 post transduction. We distinguished *bona fide* iPSC colonies from non-iPSC colonies by their morphological differences[2,17,26,27,34,35].

MEFs carrying Nanog-GFP[28] were introduced with OCT3/4, SOX2, KLF4, c-MYC and GLIS1 by retroviral transduction. Two days after infection, the medium was replaced with the mESC medium. We collected each fraction by using a SSEA-1 antibody and/or Nanog-GFP on the indicated days by flow cytometry[26]. The cells were passaged on days 7, 11, 15 and 20 at 1×10^6 cells per 100 mm dish.

PSMN differentiation. The differentiation of human ESCs/iPSCs into PSMN was performed as described previously[13]. In brief, single-cell suspensions of human

ESCs/iPSCs were plated onto fibronectin-coated plates (BD biosciences) in DMEM/F12 supplemented with 1% Insulin–Transferrin–Selenite (ITS, Life Technologies), 1% Glutamax, 1% NEAA, 2% B27 (Life Technologies), 100 nM 2-ME and 0.5% Pen/Strep. We added 3 μM CHIR99021 (Stemgent) and 50 ng ml^{-1} Activin A (Peprotech) on day 1, 3 μM CHIR99021, 25 ng ml^{-1} Activin A and 20 ng ml^{-1} bFGF on day 2 and 3 μM, CHIR99021, 10 ng ml^{-1} Activin A, 20 ng ml^{-1} bFGF and 40 ng ml^{-1} BMP4 (R&D systems) on day 3.

EN differentiation. EN differentiation was performed as described previously, with slight modification[36]. The single-cell suspensions of human pluripotent stem cells were plated onto Matrigel-coated plates in RPMI1640 (Life Technologies) containing 2% B27, 100 ng ml^{-1} Activin A, 3 μM CHIR99021 and 0.5% Pen/Strep. We added 0.5 mM sodium butyrate (Sigma) on days 1–3, and then carried out sodium butyrate-free culture until day 7.

ME differentiation. ME differentiation was performed as described previously, with slight modification[37]. The single-cell suspensions of human pluripotent stem cells were plated onto Collagen I-coated plates (BD biosciences) in DMEM/F12 containing 2% B27, 100 ng ml^{-1} Activin A, 3 μM CHIR99021 and 0.5% Pen/Strep. Forty-eight hours later, the medium was replaced with DMEM/F12 supplemented with 2% B27, 25 ng ml^{-1} BMP4 and 0.5% Pen/Strep. The medium was changed every other day until day 8.

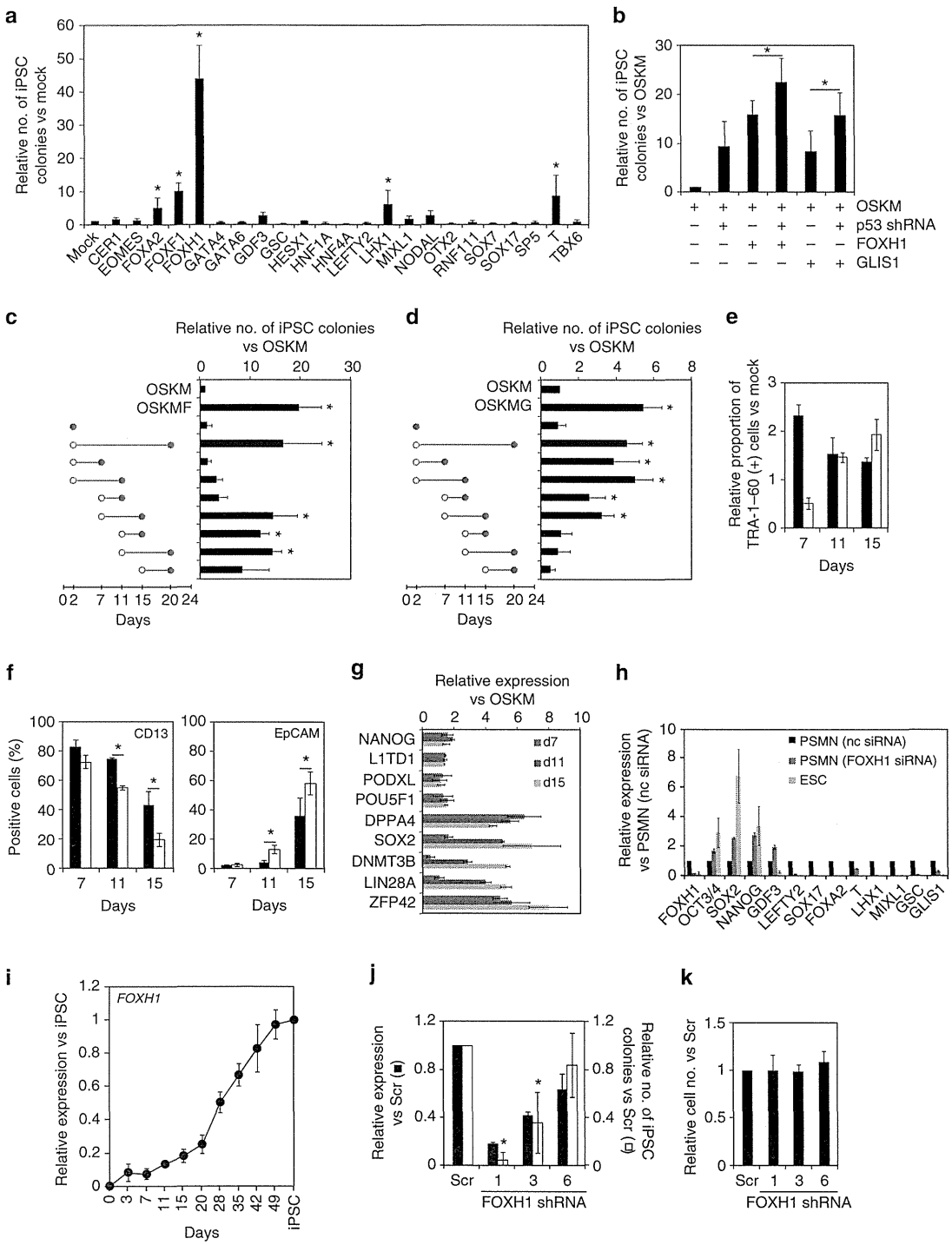

NE differentiation. NE differentiation protocol with dual SMAD inhibition was used according to previous reports[38,39]. The single-cell suspensions of pluripotent stem cells were transferred to Lipidure-coated low-binding 96-well plates (NOF corporation) in DMEM/F12 containing 5% KSR, 1% NEAA, 1% Glutamax, 100 nM 2-ME, 2 μM Dorsomorphin (Stemgent) and 10 μM SB431542 (Stemgent). The medium was changed on days 5, 8 and 11. The total differentiation period was 14 days.

Flow cytometry and fluorescence-activated cell sorting. We harvested the cells at the indicated time points by treatment with 0.25% trypsin/1 mM EDTA (Life Technologies) or Accutase (Life Technologies). Fixation and permeabilization were performed before antibody staining with 4% paraformaldehyde and 0.2% Triton X-100, respectively. At least 5×10^4 cells were analysed for quantification in all experiments using the FACS Aria II instrument (BD biosciences). Cell sorting was also performed using the FACS Aria II. We used the following antibodies for the studies: Alexa 488-conjugated TRA-1-60 (1:20, 560173, BD biosciences), Alexa 488-conjugated SSEA-4 (1:20, 506348, BD biosciences), fluorescein isothiocyanate (FITC)-conjugated TRA-2-49/6E (1:5, FCMAB133, Millipore), allophycocyanin (APC)-labelled TRA-1-85 (1:5, FAB3195A, R&D systems), APC-labelled anti-C-X-C chemokine receptor type 4 (CXCR4) antibody (1:5, FAB170A, R&D systems), PE-labelled anti-platelet-derived growth factor receptor alpha (PDGFRA) antibody (1:5, 556002, BD Pharmingen), APC-conjugated anti-BRACHYURY antibody (1:5, IC20851A, R&D systems), anti-polysialylated neuronal cell adhesion molecule (PSA-NCAM) antibody (1:50, MAB5324, Millipore), PE-conjugated CD13 antibody (1:5, 555394, BD biosciences), FITC-labelled CD326 (EpCAM) antibody (1:10, 130-080-301, Miltenyi biotec), PE-labelled SSEA-1 (560866, BD Pharmingen) and Alexa 647-conjugated anti-mouse IgM antibody (1:500, A-21238, Life Technologies).

Magnetic-activated cell sorting. The cells harvested by trypsinization were passed through a 40 μm pore size cell strainer (BD biosciences) to remove the cell debris. The cells were incubated with PE-conjugated TRA-1-60 (1:5, 560193, BD Pharmingen), and then with anti-PE microbeads (130-048-801, Miltenyi biotec). Cell separation was performed with the serial two column mode of an AutoMACS Pro system (Miltenyi biotec). After separation, we confirmed the purity by flow cytometry.

Microarray and bioinformatics. The total RNA was purified as described above, and then was evaluated using a 2100 Bioanalyzer (Agilent Technologies). Human tissue RNA panels were obtained from Clontech Laboratories. Fifty nanograms of total RNA was labelled with Cyanine 3-CTP and used for hybridization with SurePrint G3 Human GE 8 × 60 K (G4851A, Agilent Technologies) and Mouse GE 8 × 60 K (G4852A, Agilent Technologies) with the one colour protocol. The arrays were scanned with a Microarray Scanner System (G2565BA, Agilent Technologies), and extracted signals were analysed using the GeneSpring version 12.6 software programme (Agilent Technologies).

Gene expression values were normalized by the 75th percentile shifts. The hierarchical clustering analyses were performed with a Euclidean distance and complete linkage clustering method. Differentially expressed genes in each lineage were extracted by comparison with the profiles in HDFs, ESCs and iPSCs by unpaired a *t*-tests with Benjamini and Hochberg corrections (significance set at $P<0.05$, fold change > 2.0). Transiently activated or suppressed genes were narrowed down by cutting off the absolute rate of contribution in component 1 for values higher than 0.6.

The gene ontology analyses were performed using the EASE programme on the DAVID bioinformatics database website (http://www.david.abcc.ncifcrf.gov/home.jsp). The multiple protein sequence alignment was performed using the CLUSTALW programme (http://www.genome.jp/tools/clustalw/).

Gene silencing. For short-term gene silencing, Stealth small interfering RNA for FOXH1 (equal mixture of HSS189664, HSS113216 and HSS113217) or Negative control Mid GC (Life Technologies) was transfected into human ESCs/iPSCs using Lipofectamine RNAi Max (Life Technologies) according to the manufacturer's protocol on day 0 of PSMN differentiation protocol. For stable knockdown during reprogramming, we introduced a pMKO.1-puro retroviral vector (#8452, Addgene) encoding shRNA against genes of interest, at the same time as the OSKM transduction. The sequences of FOXH1 shRNA 1, 3 and 6 were 5′-CACCTCCTACT TGCCTATCTA-3′, 5′-GCCTATCTACACTCCCAATGT-3′ and 5′-TGCAGCCTG TGAGGCTCTTAA-3′, respectively.

Plasmid construction. The open reading frames of the genes used in this study were amplified by PCR, subcloned into pENTR-D-TOPO (Life Technologies) and verified by sequencing. The open reading frames were transferred to expression vectors such as pMXs-gw or pMXs-gw-IP by using the Gateway LR reaction system (Life Technologies) according to the manufacturer's protocol. To generate cGR-fused constructs, stop codon-lacking GLIS1 and FOXH1 were amplified by PCR and cloned into pCR2.1-TOPO (Life Technologies). An *Eco*RI/*Spe*I fragment of each gene cloned in pCR2.1 and a *Spe*I/*Not*I fragment of pPyCAG-cGR-IP were inserted into the *Eco*RI/*Not*I site of pMXs. A knockdown vector for human *p53* gene[40] (pMKO.1-puro p53 shRNA2, #10672) was purchased from Addgene.

Quantitative reverse transcription polymerase chain reaction. Total RNA was purified from cell lysates treated with the Qiazol reagent (Qiagen) by using a miRNeasy mini kit (Qiagen), and was incubated with the Turbo DNA free kit (Life Technologies) to remove genomic DNA. The reverse transcription reaction was performed with 1 μg of DNase-treated RNA using the ReverTra Ace-α kit (Toyobo) and oligo dT_{20} primer. PCR was performed using SYBR premix Ex-Taq II (Takara) and a StepOne instrument (Applied Biosciences). The primer sequences for each gene are provided in Supplementary Table 4.

Embryoid body formation. Small clumps of human ESCs/iPSCs were transferred to low-binding plates (Nunc) in DMEM/F12 (Life Technologies) containing 20% KSR, 1% Glutamax, 1% NEAA, 100 nM 2-ME and 0.5% Pen/Strep. The medium was changed every other day. After 8 days of floating culture, aggregates were transferred onto gelatinized plates and cultured for another eight days. The medium was changed every other day.

Western blotting analyses. Cell lysates were prepared using RIPA buffer (50 mM Tris–HCl, pH 8.0, 150 mM NaCl, 1% nonidet P-40, 1% sodium deoxycholate, and 0.1% SDS), supplemented with protease inhibitor cocktail (Roche). Thirty micrograms of denatured cell lysates were separated by electrophoresis on 12 or 14% SDS–polyacrylamide gels, and were transferred to polyvinylidene fluoride membranes (Millipore). The blot was blocked with TBST (20 mM Tris–HCl, pH 7.6, 136 mM NaCl, and 0.1% Tween-20) containing 1% skim milk and then incubated with primary antibody solution at 4 °C overnight. After washing with TBST, the membrane was incubated with horseradish peroxidase (HRP)-conjugated secondary antibody for 45 min at room temperature with constant agitation. Signals were raised with Immobilon Western HRP substrate

Figure 3 | Facilitation of the reprogramming efficiency by FOXH1. (**a**) FOXH1 facilitates iPSC generation. Shown are the relative numbers of iPSC colonies on day 24. $N=3$. *$P<0.05$ vs Mock (paired *t*-test). (**b**) The action of FOXH1 is independent of that of p53. Shown are the relative numbers of iPSC colonies on day 24. $N=3$. *$P<0.05$ (paired *t*-test). (**c**) FOXH1 enhances reprogramming in the late stage. We added 100 nM of dexamethasone (Dex) into the medium of HDFs transduced with OSKM and FOXH1GR from the time indicated by open circles until that indicated by closed circles. Shown are the relative numbers of iPSC colonies on day 24. $N=3$. *$P<0.05$ vs OSKM (paired *t*-test). (**d**) GLIS1 enhances reprogramming in the early stage. We performed same kind of experiments to Figure 3c using GLIS1GR instead of FOXH1GR. $N=3$. *$P<0.05$ vs OSKM (paired *t*-test). (**e**) FOXH1 increases TRA-1-60 (+) cells in the late stage. Shown are the relative proportions of TRA-1-60 (+) cells induced by OSKMG (closed bars) or OSKMF (opened bars). $N=3$. (**f**) FOXH1 promotes the epithelialization during reprogramming. Shown are the proportions of CD13 (+) or EpCAM (+) cells in the TRA-1-60 (+) cell population carrying OSKM (closed bars) or OSKMF (open bars) by flow cytometry. $N=3$. *$P<0.05$ (paired *t*-test). (**g**) FOXH1 enhances the expression of late reprogramming markers. Shown are the relative expression levels in TRA-1-60 (+) cells induced by OSKMF normalized to *G3PDH* expression. $N=3$. (**h**) FOXH1 is required for PSMN differentiation. Shown are the relative expression levels in PSMN differentiated from FOXH1 small interfering RNA-transduced ESCs/iPSCs normalized to *G3PDH* expression. $N=3$. (**i**) The expression of endogenous FOXH1 in TRA-1-60 (+) cells. Shown are the relative expression levels of FOXH1 normalized to *G3PDH* expression. $N=3$. (**j**) Endogenous FOXH1 is required for iPSC generation. We introduced OSKM, along with scramble shRNA (Scr) or FOXH1 shRNAs (1, 3 or 6), into HDFs. On day 15, the knockdown efficiencies were evaluated by qRT-PCR (closed bars). Each value was normalized to that of *G3PDH*. The open bars indicate the relative numbers of iPSC colonies on day 24. $N=3$. *$P<0.05$ versus Scr (paired *t*-test). (**k**) FOXH1 does not affect HDF proliferation. Shown are the relative numbers of HDFs transduced with OSKM in combination with pMKO.1-puro encoding scramble shRNA (Scr) and FOXH1 shRNA1, 3 or 6 on day 7. Each value was normalized to that of *G3PDH*. $N=3$.

(Millipore) and detected using a LAS3000 mini imaging system (FUJIFILM). Primary antibodies for p53 (1:200, sc-126, Santa Cruz), p21 (1:500, sc-397, Santacruz) and β-ACTIN (1:5,000, A5441, Sigma), and horseradish peroxidase-linked secondary antibodies for mouse immunoglobulin G (IgG) (1:3,000, #7076, Cell signalling technology) and rabbit IgG (1:2,000, #7074, Cell signalling technology) were used.

Immunocytochemistry. The cells were fixed with 4% paraformaldehyde and permeabilized with phosphate-buffered saline (PBS) containing 5% goat or donkey normal serum (Chemicon), 1% bovine serum albumin (BSA; Nacalai Tesque) and 0.2% Triton X-100 (Nacalai Tesque). Samples were incubated with primary antibodies against NANOG (1:100, RCAB003P, ReproCELL), T (1:100, AF2085, R&D systems) SOX17 (1:200, AF1924, R&D systems), α-smooth muscle actin (1:600, M085101, DAKO) and NESTIN (1:1,000, ab5968, Abcam), which were diluted in staining solution (PBS containing 1% BSA) at 4 °C overnight. After being washed with PBS, the samples were exposed to staining solution containing fluorescence-conjugated secondary antibodies such as Alexa 488-conjugated anti-goat IgG (1:500, A-11055, Life Technologies), Alexa 546-conjugated anti-mouse IgG (1:500, A-11030, Life Technologies), Alexa 488-conjugated anti-rabbit IgG (1:500, A-11034, Life Technologies) and Alexa 546-conjugated anti-rabbit IgG (1:500, A-11035, Life Technologies), as well as Hoechst 33342 (1 μg ml^{-1}, H3570, Life Technologies). Images were obtained using a BZ9000 imaging system (KEYENCE).

Pyrosequencing. Five hundred nanograms of purified genomic DNA was used for the bisulphite CT conversion with the EZ DNA methylation kit (Zymo Research) according to the manufacturer's recommendations. The resultant DNA samples were used for PCR with biotinylated primers as templates, and amplified products were analysed by the Pyromark system (Qiagen). The primer sequences are provided in Supplementary Table 4.

Chromatin immunoprecipitation. Approximately 3 × 10^5 cells were fixed with 1% formaldehyde and quenched with 125 mM glycine. Fixed cells were sequentially treated with LB1 (50 mM Hepes-KOH, pH 7.5, 140 mM NaCl, 1 mM EDTA, 10% glycerol, 0.5% Nonidet P-40 and 0.25% Triton X-100), LB2 (10 mM Tris–HCl, pH 8.0, 200 mM NaCl, 1 mM EDTA and 0.5 mM EGTA), LB3 (10 mM Tris–HCl, pH 8.0, 100 mM NaCl, 1 mM EDTA, 0.5 mM EGTA and 0.1% sodium deoxycholate) to obtain nuclear extracts. Chromatin samples were sheared by treatment with a Misonix Astrason S-3000 sonicator (On, 30 s; Off, 1 min; Power, 7.0; 15 cycles). We added 1/10 volume of 10% Triton X-100 solution to the cell lysates and obtained cleared supernatants after centrifugation. To reduce the non-specific background, we incubated the chromatin samples with normal mouse IgG (sc-2025, Santa Cruz) linked with Dynabeads M-280 Sheep Anti-Mouse IgG (102-01D, Life Technologies) for 30 min at 4 °C. After removal of the beads, the cleared lysates were incubated with a Dynabeads-conjugated anti-trimethylated lysine 4 of histone H3 antibody (MABI0304, Wako) overnight at 4 °C with constant rotation. After incubation, the beads were washed twice each with wash buffer 1 (20 mM Tris–HCl, 8.0, 150 mM NaCl, 2 mM EDTA, 1% TritonX-100 and 0.1% SDS), wash buffer 2 (20 mM Tris–HCl, pH 8.0, 500 mM NaCl, 2 mM EDTA, 1% Triton X-100 and 0.1% SDS), wash buffer 3 (10 mM Tris–HCl, pH 8.0, 250 mM lithium chloride, 1 mM EDTA, 1% Nonidet-P 40 and 1% sodium deoxycholate) and TE buffer (10 mM Tris–HCl, pH 8.0 and 1 mM EDTA). Then, we incubated the beads with elution buffer (25 mM Tris–HCl, pH 7.5, 5 mM EDTA and 0.5% SDS) supplemented with 0.4 mg ml^{-1} protease K (Nacalai Tesque) at 42 °C for 1 h, and then at 65 °C overnight with constant rotation. Eluates were purified using the Qiaquick PCR purification kit (Qiagen) and were used for PCR as templates. The primer sequences are provided in Supplementary Table 4.

Teratoma formation and histological analyses. Approximately 3 × 10^5 harvested cells suspended in DMEM/F12 containing 10 μM Y-27632 (Wako) were injected into the testes of severe combined immunodeficient male mice (6 weeks old) by using a Hamilton syringe[41]. Animal experiments were approved by Kyoto University ethical committee (Approved number is K3-12). After 8–10 weeks, the tumours were dissected and fixed with 4% paraformaldehyde and 70% ethanol in sequence. Paraffin-embedded sections were stained with hematoxylin and eosin. Images were obtained by using a BZ9000 system.

Single-cell manipulation. Single-cell suspensions prepared by trypsinization were incubated with PE-conjugated TRA-1-60 and 4′,6-diamidino-2-phenylindole (Life Technologies). TRA-1-60 (+)/4′,6-diamidino-2-phenylindole (−) cells were directly sorted onto MMC-treated SNL feeders in human ESC medium supplemented with 4 ng ml^{-1} bFGF and 10 μM Y-27632 for the colony formation assay, or into PCR master mix for the single-cell expression analyses using the FACS Aria II instrument. The template for the single-cell PCR was prepared using the Cellsdirect Reagent (Life Technologies) according to the manufacturer's protocol. Pre-amplification of the target sequences was performed for 22 cycles. The subsequent PCR and data collection were conducted with a Biomark system (Fluidgm). Each sample was validated based on the expression of either *G3PDH* or *ACTB*, with Ct value less than 15. The Ct values higher than 26 were considered to indicate no expression and were unified as 100 for the calculation of the ΔCt. The Taqman assays used in this study are shown in Supplementary Table 5.

References

1. Takahashi, K. & Yamanaka, S. Induction of pluripotent stem cells from mouse embryonic and adult fibroblast cultures by defined factors. *Cell* **126,** 663–676 (2006).
2. Takahashi, K. *et al.* Induction of pluripotent stem cells from adult human fibroblasts by defined factors. *Cell* **131,** 861–872 (2007).
3. Yamanaka, S. Elite and stochastic models for induced pluripotent stem cell generation. *Nature* **460,** 49–52 (2009).
4. Vierbuchen, T. & Wernig, M. Molecular roadblocks for cellular reprogramming. *Mol. Cell* **47,** 827–838 (2012).
5. Polo, J. M. *et al.* A molecular roadmap of reprogramming somatic cells into iPS cells. *Cell* **151,** 1617–1632 (2012).
6. O'Malley, J. *et al.* High-resolution analysis with novel cell-surface markers identifies routes to iPS cells. *Nature* **499,** 88–91 (2013).
7. Buganim, Y. *et al.* Single-cell expression analyses during cellular reprogramming reveal an early stochastic and a late hierarchic phase. *Cell* **150,** 1209–1222 (2012).
8. Andrews, P. W., Banting, G., Damjanov, I., Arnaud, D. & Avner, P. Three monoclonal antibodies defining distinct differentiation antigens associated with different high molecular weight polypeptides on the surface of human embryonal carcinoma cells. *Hybridoma* **3,** 347–361 (1984).
9. Chan, E. M. *et al.* Live cell imaging distinguishes bona fide human iPS cells from partially reprogrammed cells. *Nat. Biotechnol.* **27,** 1033–1037 (2009).
10. Tanabe, K., Nakamura, M., Narita, M., Takahashi, K. & Yamanaka, S. Maturation, not initiation, is the major roadblock during reprogramming toward pluripotency from human fibroblasts. *Proc. Natl Acad. Sci. USA* **110,** 12172–12179 (2013).
11. D'Amour, K. A. *et al.* Efficient differentiation of human embryonic stem cells to definitive endoderm. *Nat. Biotechnol.* **23,** 1534–1541 (2005).
12. Yu, P., Pan, G., Yu, J. & Thomson, J. A. FGF2 sustains NANOG and switches the outcome of BMP4-induced human embryonic stem cell differentiation. *Cell Stem Cell* **8,** 326–334 (2011).
13. Oldershaw, R. A. *et al.* Directed differentiation of human embryonic stem cells toward chondrocytes. *Nat. Biotechnol.* **28,** 1187–1194 (2010).
14. Davis, R. P. *et al.* Targeting a GFP reporter gene to the MIXL1 locus of human embryonic stem cells identifies human primitive streak-like cells and enables isolation of primitive hematopoietic precursors. *Blood* **111,** 1876–1884 (2008).
15. Panopoulos, A. D. *et al.* The metabolome of induced pluripotent stem cells reveals metabolic changes occurring in somatic cell reprogramming. *Cell Res.* **22,** 168–177 (2012).
16. Hanna, J. *et al.* Direct cell reprogramming is a stochastic process amenable to acceleration. *Nature* **462,** 595–601 (2009).
17. Hong, H. *et al.* Suppression of induced pluripotent stem cell generation by the p53-p21 pathway. *Nature* **460,** 1132–1135 (2009).
18. Marion, R. M. *et al.* A p53-mediated DNA damage response limits reprogramming to ensure iPS cell genomic integrity. *Nature* **460,** 1149–1153 (2009).
19. Li, H. *et al.* The Ink4/Arf locus is a barrier for iPS cell reprogramming. *Nature* **460,** 1136–1139 (2009).
20. Utikal, J. *et al.* Immortalization eliminates a roadblock during cellular reprogramming into iPS cells. *Nature* **460,** 1145–1148 (2009).
21. Kawamura, T. *et al.* Linking the p53 tumour suppressor pathway to somatic cell reprogramming. *Nature* **460,** 1140–1144 (2009).
22. Samavarchi-Tehrani, P. *et al.* Functional genomics reveals a BMP-driven mesenchymal-to-epithelial transition in the initiation of somatic cell reprogramming. *Cell Stem Cell* **7,** 64–77 (2010).
23. Li, R. *et al.* A mesenchymal-to-epithelial transition initiates and is required for the nuclear reprogramming of mouse fibroblasts. *Cell Stem Cell* **7,** 51–63 (2010).
24. Yamamoto, M. *et al.* The transcription factor FoxH1 (FAST) mediates Nodal signaling during anterior-posterior patterning and node formation in the mouse. *Genes Dev.* **15,** 1242–1256 (2001).
25. Hoodless, P. A. *et al.* FoxH1 (Fast) functions to specify the anterior primitive streak in the mouse. *Genes Dev.* **15,** 1257–1271 (2001).
26. Maekawa, M. *et al.* Direct reprogramming of somatic cells is promoted by maternal transcription factor Glis1. *Nature* **474,** 225–229 (2011).
27. Nakagawa, M. *et al.* Generation of induced pluripotent stem cells without Myc from mouse and human fibroblasts. *Nat. Biotechnol.* **26,** 101–106 (2008).
28. Okita, K., Ichisaka, T. & Yamanaka, S. Generation of germ-line competent induced pluripotent stem cells. *Nature* **448,** 313–317 (2007).
29. Tomoda, K. *et al.* Derivation conditions impact X-inactivation status in female human induced pluripotent stem cells. *Cell Stem Cell* **11,** 91–99 (2012).

30. Morita, S., Kojima, T. & Kitamura, T. Plat-E: an efficient and stable system for transient packaging of retroviruses. *Gene. Ther.* **7,** 1063–1066 (2000).
31. Thomson, J. A. *et al.* Embryonic stem cell lines derived from human blastocysts. *Science* **282,** 1145–1147 (1998).
32. Suemori, H. *et al.* Efficient establishment of human embryonic stem cell lines and long-term maintenance with stable karyotype by enzymatic bulk passage. *Biochem. Biophys. Res. Commun.* **345,** 926–932 (2006).
33. McMahon, A. P. & Bradley, A. The Wnt-1 (int-1) proto-oncogene is required for development of a large region of the mouse brain. *Cell* **62,** 1073–1085 (1990).
34. Okita, K. *et al.* A more efficient method to generate integration-free human iPS cells. *Nat. Methods* **8,** 409–412 (2011).
35. Nakagawa, M., Takizawa, N., Narita, M., Ichisaka, T. & Yamanaka, S. Promotion of direct reprogramming by transformation-deficient Myc. *Proc. Natl Acad. Sci. USA* **107,** 14152–14157 (2010).
36. Kajiwara, M. *et al.* Donor-dependent variations in hepatic differentiation from human-induced pluripotent stem cells. *Proc. Natl Acad. Sci. USA* **109,** 12538–12543 (2012).
37. Mae, S. *et al.* Monitoring and robust induction of nephrogenic intermediate mesoderm from human pluripotent stem cells. *Nat. Commun.* **4,** 1367 (2013).
38. Chambers, S. M. *et al.* Highly efficient neural conversion of human ES and iPS cells by dual inhibition of SMAD signaling. *Nat. Biotechnol.* **27,** 275–280 (2009).
39. Morizane, A., Doi, D., Kikuchi, T., Nishimura, K. & Takahashi, J. Small molecule inhibitors of BMP and activin/Nodal signals promote highly efficient neural induction from human pluripotent stem cell efficient neural induct stem cell. *J. Neurosci. Res.* **89,** 117–126 (2010).
40. Masutomi, K. *et al.* Telomerase maintains telomere structure in normal human cells. *Cell* **114,** 241–253 (2003).
41. Watanabe, K. *et al.* A ROCK inhibitor permits survival of dissociated human embryonic stem cells. *Nat. Biotechnol.* **25,** 681–686 (2007).

Acknowledgements

We would like to acknowledge S. Mae, M. Kotaka, M. Kajiwara, A. Morizane and J. Takahashi for guidance regarding the cellular differentiation, T. Taya and A. Watanabe for the bioinformatics analyses and H. Niwa, H. Suemori, T. Kitamura and K. Woltjen for providing valuable materials. We are also grateful to T. Ichisaka and K. Asano for technical assistance, to R. Kato, E. Minamitani, S. Takeshima, R. Fujiwara, Y. Miyake, S. Okamoto and Y. Higuchi for administrative support and to E. Rulifson and all CiRA members for helpful discussions. This work was supported in part by Grants-in-Aid for Scientific Research from The Japanese Society for the Promotion of Science; from The Ministry of Education, Culture, Sports, Science and Technology; by a grant from The Leading Project of the Ministry of Education, Culture, Sports, Science and Technology and by a grant from The Funding Program for World-Leading Innovative Research and Development on Science and Technology (First Program) of The Japanese Society for the Promotion of Science.

Author contributions

Ka.T. and Ko.T. conducted most of the experiments and the data analyses, with assistance from A.S., Me.N. and Mi.N. M.Y. performed the mouse embryo manipulation and WISH. M.O. conducted the neural differentiation and reprogramming experiments. K.S. performed the knockdown experiments. K.O. prepared the mouse differentiated cell samples. Ka.T., Ko.T. and S.Y. analysed the data. Ka.T. and S.Y. designed and supervised the project and wrote the manuscript.

Additional information

Accession codes: The microarray data have been deposited in Gene Expression Omnibus under accession number GSE50206.

Supplementary Information accompanies this paper at http://www.nature.com/naturecommunications

Competing financial interests: S.Y. is a member without salary of the scientific advisory boards of iPierian, iPS Academia Japan, Megakaryon Corporation, and Healios K.K. The remaining authors declare no competing financial interests.

Reprints and permission information is available online at http://npg.nature.com/reprintsandpermissions/

How to cite this article: Takahashi, K. *et al.* Induction of pluripotency in human somatic cells via a transient state resembling primitive streak-like mesendoderm. *Nat. Commun.* 5:3678 doi: 10.1038/ncomms4678 (2014).

2014年7月号(Vol 37 No. 8)

臨床応用に向けた再生医学研究

iPS 細胞

Induced pluripotent stem cell

安田勝太郎[*, **] 上本 伸二[***] 長船 健二[**]
Katsutaro Yasuda *Shinji Uemoto* *Kenji Osafune*

●要旨●2006年に京都大学のYamanakaらによりiPS細胞の樹立が報告されて以来，iPS細胞を用いた再生医療の研究が急速に進展し，本年秋にはわが国においてiPS細胞を用いた移植治療の臨床研究が開始される予定である。iPS細胞は無限の増殖能と全身の細胞種への多分化能をもつため，とくに深刻なドナー不足の状態が続いている肝移植，膵臓・膵島移植，小腸移植など消化器外科領域においても解決策の1つとして大いに期待されている。しかし，iPS細胞から機能的に成熟した肝細胞，膵β細胞，腸管細胞を分化誘導することや生体内に移植して機能させることはまだまだ困難であり，今後もさらなる研究の進展が期待される。

● key words：iPS細胞，ES細胞，膵臓，肝臓，腸管

はじめに

京都大学のYamanakaらのグループにより2006年にマウス，そして2007年にはヒトの線維芽細胞からiPS細胞（induced pluripotent stem cell：人工多能性幹細胞）が樹立され，患者自身の多能性幹細胞を用いた自家移植が現実味を帯びることとなった[1)2)]（図1）。その後，iPS細胞研究は急速に進展し，ついにわが国において理化学研究所のグループが，本年秋に加齢黄斑変性症患者に対し世界初のiPS細胞を用いた移植治療の臨床研究を行う予定である。

本稿では，いよいよ臨床応用の段階に入ったiPS細胞研究の現状と消化器外科領域の最新の動向を中心に解説したい。

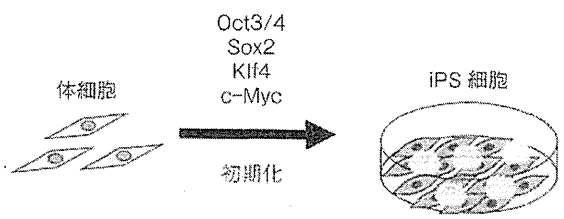

a：Yamanaka 4因子を導入することによって体細胞が初期化される

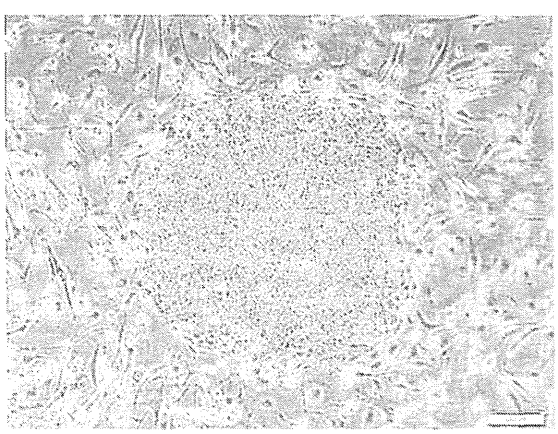

b：ヒトiPS細胞のコロニー
周囲の細胞は未分化状態を維持するためのfeeder細胞

図1 iPS細胞の樹立

* 京都大学iPS細胞研究所増殖分化機構研究部門
** 同大学大学院医学研究科肝胆膵・移植外科
*** 同教授
* 同大学iPS細胞研究所増殖分化機構研究部門准教授

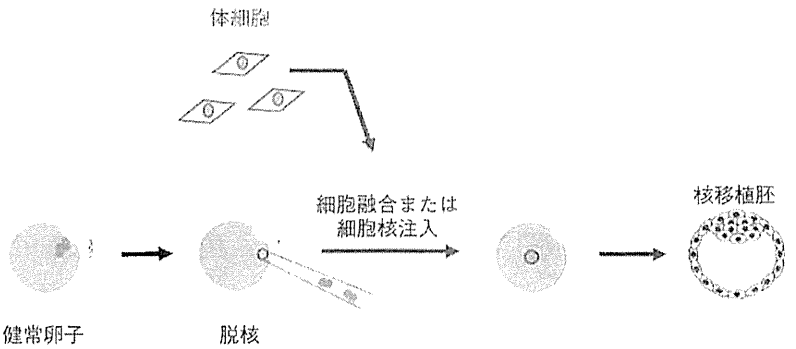

図2　体細胞核移植による初期化
体細胞核移植では，脱核した卵子と体細胞を融合させるか，脱核した卵子に体細胞核を注入することで胚が作製される。胚を構成する細胞の核は初期化された体細胞核である

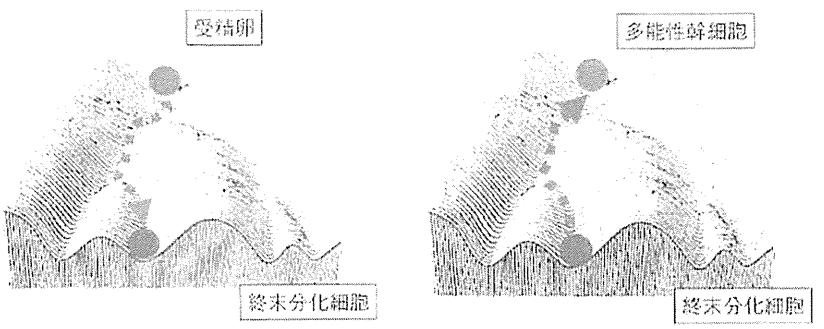

a：正常発生　　b：初期化
（体細胞核移植，細胞融合，iPS 細胞）
〔文献35）をもとに作成〕

図3　細胞の分化過程を谷間に転がり落ちるボールで表現した概念図
（Waddington's epigenetic landscape）
Gurdon らの体細胞核移植実験により，終末分化細胞の核は一定条件下で初期化されることが示された

iPS 細胞とは

1. 歴史的背景

iPS 細胞開発からわずか6年後の2012年に，Yamanaka はノーベル生理学・医学賞を受賞した。その受賞理由は，「成熟した細胞を，多能性をもつ細胞へと初期化できることを発見した」である。生物の個体はたった1つの受精卵から始まる。それが分裂を繰り返しさまざまな細胞系譜に分化しつつ，組織や臓器，そして個体が形成される。通常，最終分化した細胞は受精卵がもつようなさまざまな細胞に分化し得る多分化能（多能性）を再度発揮することはない。終末分化細胞が多能性を発揮しない理由は長らく大きな疑問であった。1958年に，英国の Gurdon（2012年ノーベル生理学・医学賞共同受賞者）らはクローンガエルを作製することに成功した[3]。同グループは，核を除いたアフリカツメガエルの未受精卵に，オタマジャクシの体細胞核を移植すること（体細胞核移植：somatic cell nuclear transfer）により受精卵を作製した。これは体細胞核が初期化（reprogramming）されたことを意味する（図2）。また，体細胞と ES 細胞（後述参照）の細胞融合によっても体細胞核の初期化が生じることが京都大学の Tada らによって示された[4]。これらの知見から，終末分化細胞は多能性を喪失したわけではなく潜在的に保持していること，および，受精卵や ES 細胞の細胞質に初期化誘導因子が存在することが示唆された。Yamanaka らはこの初期化誘導因子（Yamanaka 4 因子：Oct3/4, Sox2, Klf4, c-Myc）を同定し，これらをマウスおよびヒト線維芽細胞に導入することで，線維芽細胞を初期化することに成功したのである（図3）。

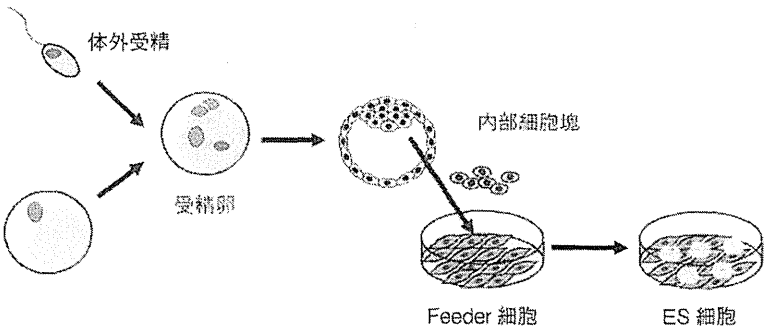

a：不妊治療のため体外受精を行った受精卵のうち，余剰胚の内部細胞塊を摘出し，ヒトES細胞が樹立される

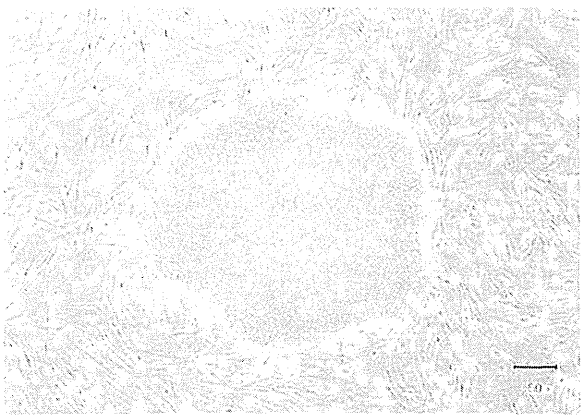

b：ヒトES細胞のコロニー
ヒトiPS細胞と外観は同じである。コロニー周辺の細胞は未分化状態を維持するためのfeeder細胞

図4　ヒト胚からのES細胞樹立

2. iPS細胞の特長

1) 無限の増殖能と多分化能

1998年に米国ウィスコンシン大学のThomsonらによりヒトES細胞（embryonic stem cell：胚性幹細胞）の樹立が報告された[5]。ES細胞は着床前の受精卵胚盤胞の一部である内部細胞塊を採取，培養することによって樹立される（図4）。ES細胞は，無限の増殖能と全身のすべての細胞種に分化できる多分化能を有していることが特長である。iPS細胞は，このようなES細胞とほぼ同等の増殖能と多分化能を備えているため，移植医療の細胞源として注目されている。

2) 倫理的問題の回避

ES細胞は不妊治療としての体外受精の際に作製された受精卵のうち，余剰胚を用いて樹立される。つまり，生命の萌芽であるヒト胚を破壊して樹立されるため，倫理的問題が存在する。一方，iPS細胞は体細胞から作製されるため，このような倫理的問題は回避される。

3) 拒絶反応の回避

iPS細胞は患者自身の体細胞から樹立されたものを用いる場合には，理論上，拒絶反応は生じないはずである。しかし，2011年に米国カリフォルニア大学のグループがiPS細胞を用いた自家移植において拒絶反応が生じるとする論文を発表し，話題となった[6]。ただ，この論文では未分化なマウスiPS細胞をそのまま同系統のマウス皮下に移植し，形成された奇形腫に対する免疫原性を観察している。そもそも未分化なiPS細胞を移植医療に用いることはなく，拒絶反応も形成された腫瘍に対する免疫反応をみていることから，当初よりその結論に対し疑問が投げかけられていた。その後，2013年に放射線医学総合研究所のAraki，Abeらと鶴見大学のNifujiらのグループにより，マウスiPS細胞から得られた皮膚および骨髄細胞を同系統のマウスに移植しても拒絶反応を生じないことが報告された[7]。また同年，京都大学のTakahashi，Morizaneらはカニクイザルからの iPS細胞を樹立し，そこから分化誘導させた神経細胞を同一のサルに自家移植したところ，拒絶反応を認めなかったことを報告している[8]。

臨床応用に向けた安全で効率的なiPS細胞樹立法の開発

iPS細胞開発当初から，将来の臨床応用に向けて，悪性腫瘍形成のリスクなどの問題点が指摘されてき

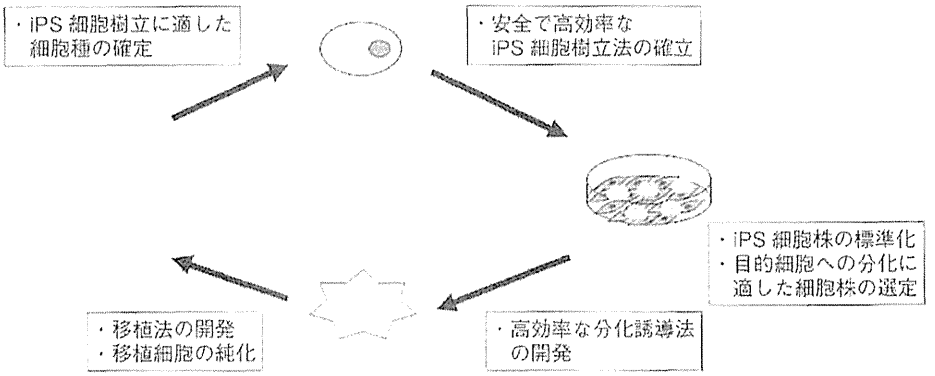

図1 iPS 細胞の臨床応用に向けた課題
iPS 細胞の高効率な樹立法や目的細胞への高効率な分化誘導法の開発に加え，異種成分を含まない培養法やホストゲノムを損傷しない iPS 細胞樹立法の開発といった安全面に関する研究も進められなければならない

た。しかし，それらの問題点は iPS 細胞研究の急速な進展のなかですでに克服されつつある（表1）。

1. 初期化因子

Yamanaka らのグループが2006年にマウス iPS 細胞の樹立を報告した際に用いた初期化因子は Oct3/4，Sox2，Klf4，c-Myc である。このうち Klf4 と c-Myc は癌原遺伝子であり，これらを代替できる因子の研究が進められている。また，より効率的に初期化できる新規因子の探索も進められている。

1) L-Myc

c-Myc は癌原遺伝子であり，ホストゲノムに挿入されると腫瘍形成のリスクを高める。京都大学の Nakagawa らは，c-Myc を除いた3因子のみでもマウスおよびヒト iPS 細胞が樹立できることを示した[9]。しかし，iPS 細胞樹立効率が大きく低下してしまったため，次に Nakagawa らは Myc 遺伝子ファミリーの1つである L-Myc に着目した。L-Myc は増殖細胞における形質転換活性が低いことが知られているからである。c-Myc のかわりに L-Myc を用いたところ，c-Myc よりも効率的にヒト iPS 細胞を作製することができた[10]。

2) Glis1

体細胞核移植では iPS 細胞樹立よりも効率的に体細胞核を初期化できる。そこで，京都大学の Maekawa，Yamanaka らは，未受精卵および受精卵に発現する転写因子に注目し，iPS 細胞樹立効率を大きく改善させる転写因子 Glis1 を同定した[11]。さらに，Yamanaka らは，Glis1 が完全に初期化された iPS 細胞のみを増殖させ，初期化が不完全な細胞の増殖を抑制することを示した。

3) 化合物を用いた樹立

iPS 細胞樹立に有利な遺伝子の探索と同時に，遺伝子導入と置き換えることができる化合物の探索も行われている。米国ハーバード大学の Melton らのグループは，OCT3/4+SOX2+バルプロ酸の組み合わせでヒト iPS 細胞を樹立した[12]。バルプロ酸はてんかんの治療薬として一般臨床において使用されている薬剤である。また，米国スクリプス研究所の Ding らのグループは，Oct3/4+Klf4の遺伝子導入に加えて2種の化合物（BIX01294+BayK8644）の組み合わせでマウス iPS 細胞を樹立した[13]。化合物を用いた樹立法であれば，初期化遺伝子のホストゲノムへの挿入の問題は解決される。また，遺伝子導入やタンパク質・サイトカインを用いる方法と比較して，化合物は一般に安価で安定しており，培地に添加するだけであるので手技的にも簡便である。ただし，その一方で発癌性など化合物の安全性については十分な検討が必要である。

2. 遺伝子導入法（表1）

Yamanaka らのグループは iPS 細胞樹立のオリジナルの論文のなかで，レトロウイルスベクターを用いて遺伝子導入を行っている。レトロウイルスベクターは，ホストゲノムに組み込まれることで目的遺伝子を発現させる。しかし，1999年にフランスで X-SCID（X 連鎖重症複合免疫不全症）患者に対するレトロウイルスを用いた遺伝子治療が行われたが，ホストゲノムへのベクター挿入により癌原遺伝子が過剰発現し，白血病が発症するという重篤な合併症が生じた[14]。したがって，実際の医療に使用する iPS 細胞の樹立には，

表1　さまざまなiPS細胞樹立法

		ホストゲノムへの挿入
ウイルス	レトロウイルス	○
	レンチウイルス	○
	アデノウイルス	×
	センダイウイルス	×
DNA	エピソーマルプラスミド	×[a]
	Cre-loxP システム	△[b]
	トランスポゾン	△[b]
RNA	合成改変 mRNA	×
	合成 microRNA	×
タンパク質		×
化合物		×

現在までにホストゲノムへの初期化遺伝子の挿入を回避するさまざまなiPS細胞の樹立法が報告されている
a：ホストゲノムへの挿入がないことの確認が必要
b：いったんホストゲノムに挿入されたDNAを除去する操作が必要

ホストゲノムにベクターが挿入されない方法を選択しなければならない。そして，現在までにさまざまな手法が開発されているが，その多くはレトロウイルス法と比較し，樹立効率が低いことが問題となっている。

1）ホストゲノム挿入の危険性の少ないウイルスベクターの利用

2009年にDNAVEC社のFusakiらは，センダイウイルスベクターを用いたiPS細胞樹立法について報告した[15]。センダイウイルスはRNAウイルスであり，ホストゲノムに挿入されない。

2）エピソーマルプラスミド

2011年に京都大学のOkitaらは，エピソーマルプラスミドを用いたiPS細胞の樹立を報告した[16]。エピソーマルプラスミドは，細胞分裂に同調して染色体外で自己複製していくDNA配列であり，導入遺伝子がホストゲノムに挿入されずに発現が維持される。さらに，c-MycをL-Mycで置き換え，LIN28およびp53-knockdown(p53-shRNA)を加えた6因子(OCT3/4, SOX2, KLF4, L-MYC, LIN28, p53-shRNA)を用いることで，レトロウイルスを用いた場合と同等の樹立効率を実現した。現在，京都大学iPS細胞研究所およびその関連施設での再生医療の臨床研究は，主にこのエピソーマルベクター法で樹立されたiPS細胞の使用が予定されている。

3）合成改変mRNA

初期化因子をmRNAの形で細胞に導入する方法である。米国ハーバード大学のグループは，mRNAの一部を改変して安定させ，さらにI型インターフェロンを阻害する物質を加えてmRNA導入細胞の生存率を高めることで樹立効率を向上させた[17]。

4）合成microRNA

大阪大学のMoriらのグループは，マウスES細胞およびマウスiPS細胞に発現しているmicroRNA(miRNA)を解析し，初期化に必要な3種類のmiRNA(mir-200c, mir-302s, mir-369s)を同定した。そして，それらをマウスおよびヒト体細胞に導入して初期化することに成功した[18]。

3. xeno-free培養システム

移植医療を行う際に，移植細胞もしくは組織に異種動物の成分が含まれることは，既知もしくは未知の感染症や，アレルギーなどのリスクを高める。したがって，初期化する細胞の採取・培養からiPS細胞の樹立・維持・分化誘導に至るまで，可能な限り異種成分を含まない(xeno-free)培養条件が選択されなければならない。現在，さまざまな研究機関からxeno-free条件下での培養法確立の報告がなされてきた

安全な移植細胞と移植部位の選択

実際にiPS細胞から目的細胞種へ分化誘導する際，その分化誘導効率は100%ではない。つまり，培養皿

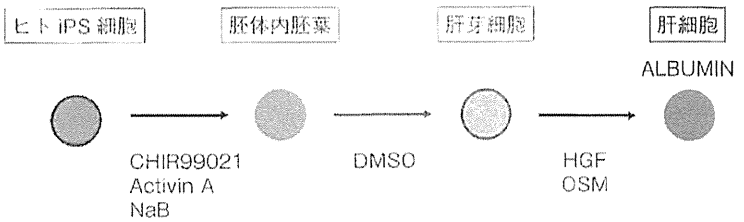

a：iPS細胞から肝細胞への分化誘導の概念図
発生過程を模倣し，各段階で適切なサイトカインや化合物を加えることで分化誘導を行う。ここでは当研究室の1例〔文献36)の分化誘導法を一部改変〕をあげる

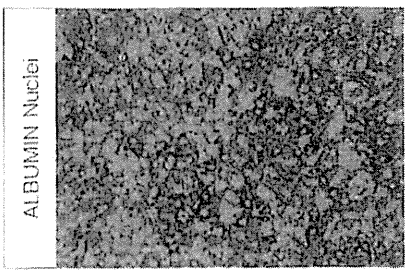

b：ヒトiPS細胞から分化誘導された肝細胞の抗アルブミン免疫染色像

図7　iPS細胞から肝細胞への分化誘導

の中には目的細胞種以外に，未分化なiPS細胞や，分化段階がより早期の未熟な細胞なども混在する。これらの細胞が移植時に混入すると，奇形腫などの腫瘍形成のリスクになる。そのため，どのようにして移植細胞を純化するかが問題となる。また，移植前だけでなく，移植後も重要である。万が一，移植細胞が腫瘍化した場合に，安全に除去できるような都合のよいものはあるか？　たとえば，本年秋に臨床研究を予定している加齢黄斑変性症の場合，ヒトiPS細胞から網膜色素上皮に分化誘導し移植を行う。分化誘導により得られる網膜色素上皮は褐色なので他の細胞と容易に区別できる。さらに，腫瘍化しても，レーザー光で対応できる。また，京都大学iPS細胞研究所が主導しているParkinson病の細胞移植治療の場合は，目的細胞であるドーパミン神経前駆細胞をその細胞表面に発現する抗原であるCORINに対する抗体を用いたセルソーティングにより選別・純化してから移植を行う[20]。さらに，腫瘍化した場合にはガンマナイフなどで対応できる。

消化器外科領域の最新の動向

1．肝　臓

種々の先天性肝疾患や肝硬変・肝不全患者に対しての唯一の根治的治療法は肝移植であるが，世界的にドナー不足の状態にある[21]。そのような状況のなかで，肝細胞移植が肝移植までの橋渡し的な役割を果たす治療法（bridging therapy）と考えられている。たとえば，先天性肝疾患のなかには脳に障害が出る前の出生後できるだけ早期に肝移植を行うべき症例もあるが，実際は新生児の小さな体に適したドナー肝臓が準備できないため，ある程度成長するのを待たなければならない。2013年8月に国立成育医療研究センターにて，凍結保存された肝細胞が生後11日の新生児に移植された。新生児への肝細胞移植は国内初である。しかし，肝細胞移植もドナーが不足している点は肝移植と同じである。そこで，細胞源としてiPS細胞が注目されている。

1）　肝細胞への分化誘導法の開発

iPS細胞から肝細胞への分化誘導は，生体内の発生過程を模倣して行われることが多い。すなわち，iPS細胞→胚体内胚葉→肝芽細胞→肝細胞といった段階を踏み，それぞれの段階で適切なサイトカインや化合物で処理することで分化させていく（図6）。報告にもよるが，分化誘導効率はアルブミン陽性細胞率でおおむね70～90%である[22]。しかし，iPS細胞から機能的に成熟した肝細胞は分化誘導できるのか？　2010年に米国カリフォルニア大学のWillenbringらのグループは，FAH（fumarylacetoacetate hydrolase：フマリルアセト酢酸ヒドラーゼ）欠損マウスの受精卵胚盤胞に正常なマウスiPS細胞を注入しキメラマウスを作製することによって，ホストマウス体内で注入したiPS細胞を肝細胞に分化させ，ホストの肝細胞を置き換えることに成功した（図7）[23]。このiPS細胞由来肝細胞を含むマウスの肝臓は正常に機能したため，生体内（*in vivo*）の環境を利用すればiPS細胞から機能的肝細胞が得られることが証明された。しかし，肝発生を模倣したさまざまな分化誘導法が報告されているが，iPS細胞から培養皿上（*in vitro*）で生体内のヒト肝細胞に匹敵する機能をもった成熟肝細胞を分化誘導することはいまだに実現していない。

2）　移植法

前述のように，ヒトiPS細胞から肝細胞へ培養皿上で分化誘導を行った報告は多数あるが，それらのiPS細胞由来肝細胞を免疫不全マウスの肝臓に移植を行

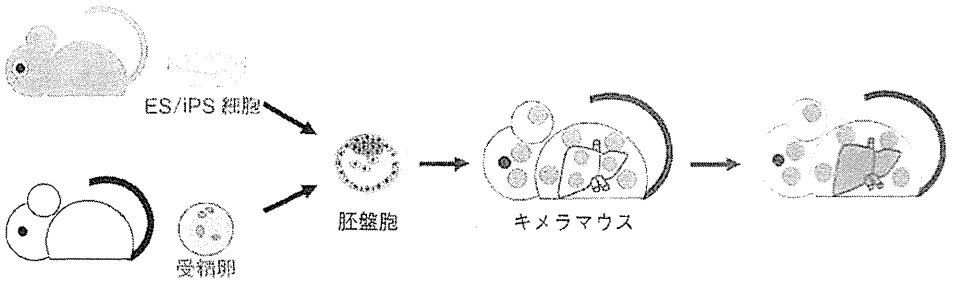

〔文献23)より引用〕

図7　キメラマウスを用いたマウス体内での成熟ヒト肝細胞の作製
マウス受精卵胚盤胞に別のマウスのES/iPS細胞を注入すると，誕生するマウスは臓器の一部に注入されたES/iPS細胞由来の細胞をもつキメラマウスとなる。FAH(fumarylacetoacetate hydrolase：フマリルアセト酢酸ヒドラーゼ)欠損マウスは生後肝細胞が障害されて死亡する。FAH欠損マウスの胚盤胞に正常なマウスiPS細胞を注入すると，ホストマウスの肝細胞は脱落していく一方で，iPS細胞由来の肝細胞が増殖して置換するため，生存することが可能になる

い，生着した報告は非常に少数である。さらに，マウス血中に移植細胞由来ヒトタンパク質（アルブミン，α_1アンチトリプシンなど）を検出した報告はより少なく，iPS細胞から作製した肝細胞を移植し機能させることは一般的に困難である。その主な理由として，2点が考えられる。1点は，単一細胞への解離操作による移植細胞へのダメージである。マウスへの肝細胞移植は，通常，経門脈的（脾注）に行われる。その際，門脈塞栓のリスクを考慮し，移植細胞を十分に解離させるが，分化誘導した肝細胞は，細胞解離のための酵素処理や物理的刺激に非常に弱い。もう1点は，分化誘導した細胞が十分に成熟していないことである。実際，免疫不全肝障害モデルマウスに対し，ヒト成熟肝細胞を脾注すると，マウス肝臓に容易に生着する。しかし，iPS細胞由来肝細胞は未成熟で，接着因子の発現が不十分であることなどの理由のため，生着率が低下することが考えられる。

この問題の解決に向けて，2013年に横浜市立大学のTaniguchiらのグループから画期的な報告がなされた[24]。Taniguchiらは，発生期の肝芽組織の形成をめざし，ヒトiPS細胞から分化誘導した肝芽細胞と，血管内皮細胞，間葉系幹細胞の共培養を行った。その結果，それらの細胞は自己組織化を起こし，血管網を伴う細胞塊を形成した。さらに，この細胞塊を免疫不全マウスの腸間膜など血流が豊富な部位に移植すると，ホストと移植細胞塊内の血管がつながり細胞塊の中に血流が形成され，代謝機能を発揮することも示された。つまり，ヒトiPS細胞由来の機能的な異所性肝組織の作製に成功したのである。今後，臨床応用に向けたヒトiPS細胞由来肝細胞・肝組織の移植法の開発が加速すると思われる。

3)　遺伝子治療

先天性代謝異常症の患者からiPS細胞を樹立しても，原因である遺伝子異常は保持される。その点を利用して疾患モデルを作製することは可能であるが，自家移植には使用できない。患者由来iPS細胞から肝細胞を分化誘導しても，その肝細胞も代謝異常を有しているからである。英国サンガー研究所のYusaらのグループは，α_1アンチトリプシン欠損症患者からiPS細胞を樹立し，遺伝子改変技術を用いて遺伝子異常を修復した。さらに，修復したiPS細胞から分化誘導された肝細胞が正常のα_1アンチトリプシンを産生することを示した[25]。これは，遺伝性疾患であってもiPS細胞の遺伝子治療により自家移植が可能になることを示唆する重要な研究成果である（図8）。

2.　膵　臓

現在，1型糖尿病をはじめとして，インスリン療法を用いても血糖コントロールがきわめて困難なインスリン依存状態の糖尿病患者に対し，膵臓・膵島移植が行われている[26]。膵臓移植は良好なインスリン離脱率と治療成績を残しているが，開腹手術であるため膵液瘻や膵炎といった合併症の危険性もある。一方，膵島移植は，経皮経肝的にカテーテルを門脈まで進めて移植を行うため侵襲は小さい。また，インスリン離脱には複数回の移植が必要であるが，インスリン離脱がで